Review

Liang Hu, Weihong Qi* and Yejun Li

Coating strategies for atomic layer deposition

https://doi.org/10.1515/ntrev-2017-0149
Received June 1, 2017; accepted August 6, 2017; previously published online September 9, 2017

Abstract: Atomic layer deposition (ALD) is a vapor phase technique capable of producing a variety of materials. It consists of the alternation of separate self-limiting surface reactions, which enables accurate control of film thickness at the Angstrom level. ALD becomes a powerful tool for a lot of industrial and research applications. Coating strategies are the key for ALD; however, there are few systematic reviews concerning coating strategies for ALD. This review provides a detailed summary of state-of-the-art coating strategies in ALD, emphasizing the recent progress in the fabrication of novel nanostructures. The progress in coating strategies is reviewed in three parts: template-assisted preparation of low-dimensional nanomaterials and complex nanostructures; surface treatments, including the surface activation and the surface blocking ways; enhanced reactor, such as plasma and fluid bed reactor, and improved growth method such as the ABC-type model. In addition, we also discussed the challenges facing the coating method for ALD.

Keywords: atomic layer deposition; coating strategy; nanostructured materials.

1 Introduction

Atomic layer deposition (ALD) is a gaseous thin-film deposition technique based on self-limiting saturated reactions [1–3]. Films with precisely controlled thickness are deposited through the repetition of ALD cycles. This technique originates from the research conducted by scientists of the former Soviet Union in the 1960s [4]. It was developed by Suntola and co-workers in the 1970s, for depositing ZnS films [5]. This technique was originally called atomic layer epitaxy (ALE), which was renamed as ALD in the mid 1990s [4, 6, 7].

As a film-coating technique, ALD is viewed as a variation of chemical vapor deposition (CVD) [8]. In a typical CVD reaction, the gas precursors are co-introduced into the chamber to undergo a heterogeneous reaction. The gaseous reaction by-products are removed by the purge of gas flow. This heterogeneous reaction often results in non-uniform thickness or non-conformal growth on most substrates [9]. Similar to CVD, ALD relies on the reaction of volatile precursors, and they share the similar precursor compound [10], except for the two separate precursors and the self-limiting film. In ALD, alternate pulsing of precursor and reactant gases are separated by purge steps to achieve self-limiting surface reactions [11]. The ALD reaction is terminated when all the available reactive surface sites are occupied, regardless of the temperature and flux of precursors. This feature is referred to as self-limiting [12], which enables ALD to deposit uniform films with high conformality and accurately controlled thickness on all kinds of substrates [11, 13]. However, to ensure the self-limiting nature of ALD, the deposition temperature should be held at a specific range. As illustrated in Figure 1A, there exists a temperature window in which the growth rate (growth per cycle, GPC) [15] is constant when the precursors are fully adsorbed to the surface of substrate. This temperature window and the consistent GPC make ALD an ideal tool to deposit films with robustness to temperature and control over thickness, while for CVD, the growth rate is strongly influenced by temperature. It follows an Arrhenius-type relation, namely, that the growth rate increases exponentially with temperature.

This temperature window in ALD ensures the consistent GPC to some extent, but on the other hand, it may constrain the feasibility of particular deposition processes [16], as shown in Figure 1B. At relatively low temperatures, the precursor may condensate and mix with the previous reactant, losing the self-limiting feature and, subsequently, leading to the heterogeneous CVD reaction. In addition, the low temperature decreases the reaction rate, which may be too low to reach the required activation energy for the reaction, while a high reaction temperature may cause the precursor to detach or even decompose

***Corresponding author: Weihong Qi,** School of Materials Science and Engineering, Central South University, Changsha, Hunan 410083, China, e-mail: weihong.qi@gmail.com; qiwh216@csu.edu.cn
Liang Hu: School of Materials Science and Engineering, Central South University, Changsha, Hunan 410083, China
Yejun Li: Hunan Key Laboratory of Super Microstructure and Ultrafast Process, School of Physics and Electronics, Central South University, Changsha, Hunan 410083, China

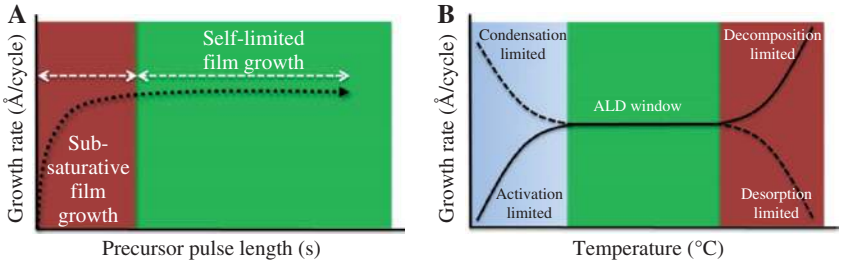

Figure 1: (A) Saturative precursor dose at the surface; (B) ALD window. Reprinted with permission from Ref. [14]. Copyright 2013 Elsevier B.V.

before reacting with another precursor, thus, destroying the self-limiting characteristics of ALD. Therefore, these precursors must have sufficient thermal stability and must not decompose at the same time during film growth in ALD. However, it is always difficult to try selecting more reactive precursors and choosing a relatively wide temperature window to ensure enough room for adsorption, which is also the key for the development of precursors.

The idealized binary ALD process is illustrated in Figure 2. It involves two sequential alternating pulses of gaseous precursors to form a thin-film product. The separated sequential gas-surface reactions are referred to as "half-reactions" [17]. Each half-reaction typically consists of two steps. For example, during the first half-reaction, a self-limiting saturated adsorption process takes place. The exposed precursor, which forms no more than one monolayer at the surface, is expected to fully react with active sites on the substrate (step 1a). Subsequently, an inert carrier gas (typically N_2 or Ar) is purged into the chamber to blow out any excess precursor or gaseous by-products, to ensure that the reaction is self-limiting (step 1b). This is followed by the second half-reaction (step 2a and step 2b), which resembles the first half-reaction. The two half reactions create up to one monolayer of the desired material and regenerate active sites for the next reaction cycle. The whole ALD process is repeated in a cyclic manner to achieve the desired film thickness. However, as the large molecular groups or generated by-products are not completely removed, the ALD growth rate per cycle is less than a full monolayer. This steric hindrance effect is avoided when a uniform film is the desired production, and sometimes, it is needed when nanoparticle formation is needed.

Although the self-limiting nature enables the ALD films with accurate thickness control, this down to nanometer thickness control limited its applications in the commercial utilization for the relatively slow growth rate of ALD films in the earlier stage [18]. Driven by the need for thinner, more controlled film growth techniques in the semiconductor industry, the interest in ALD research has been increasing rapidly. The slow deposition rate of ALD is no longer a hindrance as traditional coating processes are unable to meet the requirements of depositing highly thickness-controlled films. In recent years, thin-film deposition of various materials has made ALD a hot topic in the many fields, such as microelectronics [19, 20], catalysis [21], and energy [22–25]. As an advanced nanotechnology for thin films with conformal layer features, ALD is particularly suitable for dealing with issues in interfacial chemistry at atomic and nanometer scale. In addition, ALD has shown great potential in the construction of complex nanostructured materials that are difficult to obtain by other processing techniques, such as

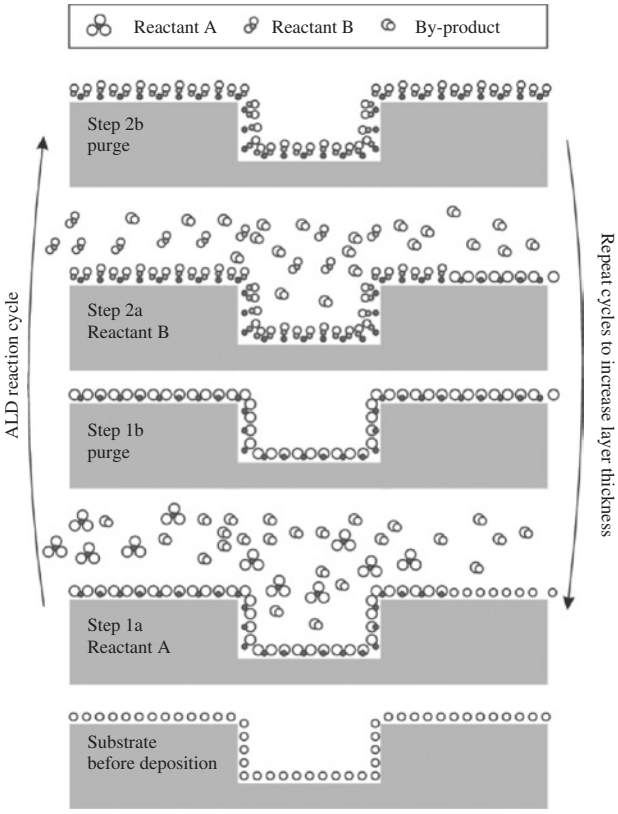

Figure 2: Schematic illustration of one ALD cycle. Reprinted with permission from Ref. [7]. Copyright 2013 AIP Publishing.

hydrothermal process, pulsed laser deposition, and CVD. This excellent film-deposition technique is often used to enhance the stability of functional material surfaces [26, 27] or to improve the properties of material interfaces [28], and it is suitable for almost all substrates of different sizes and complexities. What is more, the available materials for ALD have been greatly expanded in the recent years. To date, more than 1000 ALD processors [29] have been explored including almost the whole periodic table, i.e. oxides, nitrides, sulfides, and metals (Figure 3). In addition, newly surged materials such as gold [31] had been exemplified by ALD, which is not included in this table. These studies have greatly promoted the development of ALD technology and nanomaterials, as well as its applications.

In this rapidly developing field, there are many reviews about ALD in the literatures. Fang et al. [32] reviewed the theoretical design of ALD precursors and predicted many properties of precursors, such as the bond strength between the metal and the ligand, the thermolysis energy and barrier, the chelation energy, the hydrolysis energy, the formation energy, and so on. Ma et al. [33] reviewed the application of ALD in the deposition and surface modification of electrode materials with various nanostructures, such as deposition of solid-state electrolyte and fabrication of electrochemical catalysts. Gougousi [34] provided an overview of ALD of metal oxides on III–V semiconductor surfaces. It shows that the interface reaction leading to the formation of a sharp gate oxide/semiconductor interface is related to the surface chemistry and the transport of the surface oxides through the growing dielectric film. O'Neill et al. [29] highlighted the different ways that ALD has been utilized to design catalysts with improved activity, selectivity, and stability under a variety of conditions (e.g. high temperature, gas and liquid phase, and corrosive environments). Niu et al. [35] focused on the fabrication of nanostructured photoelectrodes, surface sensitization, and band-structure engineering of solar cell materials. McDaniel et al. [36] reviewed the research of perovskite oxides and the monolithic integration of perovskite oxides with semiconductors through ALD. Tynell and Karppinen [37] presented an overview of ALD ZnO and its applications. Wen et al. [38] highlighted the recent progress of the ALD application and processing in energy conversion and storage devices. Knoops et al. [39] discussed the ALD for nanostructured lithium (Li)-ion batteries for its capability of depositing ultrathin films in complex structures. All in all, it is suggested that coating strategies are important for atomic layer deposition; however, there is no systematic reviews on coating strategies for ALD yet. In this work, we will give a comprehensive review on the coating strategies for ALD (with emphasis on nanostructured materials), including the different dimensional nanostructure fabricated with templates, surface treatments to activate the ALD reaction and realize selective deposition, and the modifications to ALD reactor and the improvement to ALD reaction. We believe that this review will be meaningful to facilitate the application and development of ALD Technology.

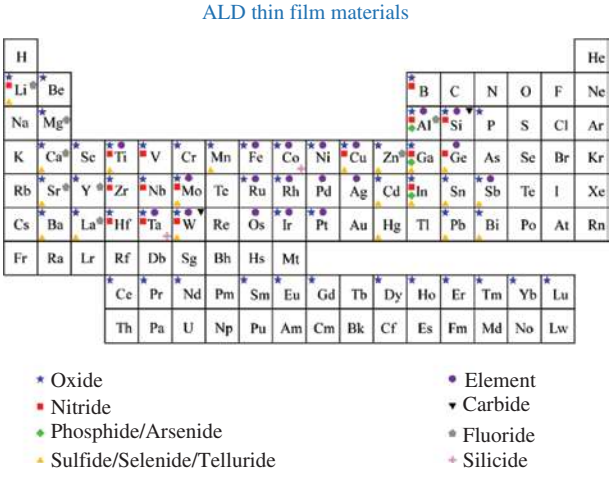

Figure 3: Overview of elements used for ALD materials. Reprinted with permission from Ref. [30]. Copyright 2016 Elsevier B.V.

2 Template-assisted nanostructure preparation

Template is one of the most effective ways for the synthesis of nanostructured materials. This tool uses a pre-defined mold to guide the formation of desired nanostructures that are difficult to obtain by other ways. In this case, ALD is a powerful tool to reproduce the complex structure, ascribed to the easy penetration of the precursors into complex structures and its self-limiting nature of ALD. With proper support, ALD has proven to be very valuable in applications that demand conformal coverage of films inside complex geometries and three-dimensional (3D) nanostructures. This template-based ALD method offers a fast and controllable advanced way as it provides a route for the synthesis of various nanostructured materials [40].

2.1 Zero-dimensional nanomaterials

The fabrication of low-dimensional materials is one of the key requirements for nanofabrication technology. Because

of the high conformality of ALD films on complex structures with precise thickness control, the nanocoating has emerged as an important application of ALD. It is particularly interesting as the nanocoating can change the optical, chemical, and mechanical properties of the nanoparticles. For example, titanium dioxide (TiO_2) ALD layer is used for protective coating of Si-based anodes for high-energy Li-ion batteries [41]. As the TiO_2 buffer layer effectively affords Si volume changes inside the spheres during the repeated charge-discharge process, the aggregation of Si particles was greatly suppressed. Therefore, high conductivity without sacrificing structural properties was achieved. Further fine tuning the film structure by post-annealing is supposed to stabilize the nanoparticles with accessibility to the surface sites and contributes to the formation of bimetallic materials. For instance, O'Neill et al. [42] confirmed that high-temperature treatment opens porosity in the overcoat by forming crystallites of γ-Al_2O_3 on Cu nanoparticles. This ALD overcoat on copper shows remarkable stability by selective armoring the under-coordinated copper atoms on the nanoparticle surface. Lu and co-workers [26] further verified it by annealing the Pd catalyst at a high temperature after the Al_2O_3 coating. The diffuse reflectance infrared spectra of CO clearly indicated that the Pd catalyst with ~8-nm ALD Al_2O_3 overcoats became porous after the high-temperature treatment, which contained ~2-nm pores after activation as depicted by the model in Figure 4C. Tests showed that the porous Al_2O_3 film selectively blocked the edge and corner atoms of Pd particles, and separated the catalyst and the reaction product, while keeping the catalyst surface accessible. As pictured in Figure 4D, the porous Al_2O_3 overcoat trapped and stabilized the Pd NPs, inhibiting Pd NP leaching and coke formation, which greatly enhanced ethylene formation. While for the uncoated Pd/Al_2O_3 catalyst during oxidative dehydrogenation of ethane (ODHE) reaction, the filamentous carbon (thick black lines) plugged the reactor, and there was substantial sintering and leaching of Pd NPs from the support (barred white lines), as pictured in Figure 4B. Thus, the catalyst clearly inhibited coke formation and improved the thermal stability of Pd NPs at high temperature. Ramachandran et al. [43] further utilized the energy provided by thermal treatment to rationally design and tailor bimetallic catalysts. They first deposited a Pt/In_2O_3 bilayer by ALD and then thermally treated the bilayer in hydrogen. The ALD-deposited bilayer transformed into alloyed Pt-In particles because of atomic migration and coalescence at the support surface. This established a new way for fully tailored synthesis of bimetallic nanoparticles, with accurate control over particle size and alloy composition by changing the thickness of the ALD-grown Pt/In_2O_3 bilayer.

Because of the high surface area of 0D nanoparticles, the duplication of the particle structures is particularly interesting. With a sacrificial carbon nanosphere template (Figure 5), Hong and Sang [40] fabricated nanocrystalline anode materials made of mesoporous anatase TiO_2. They

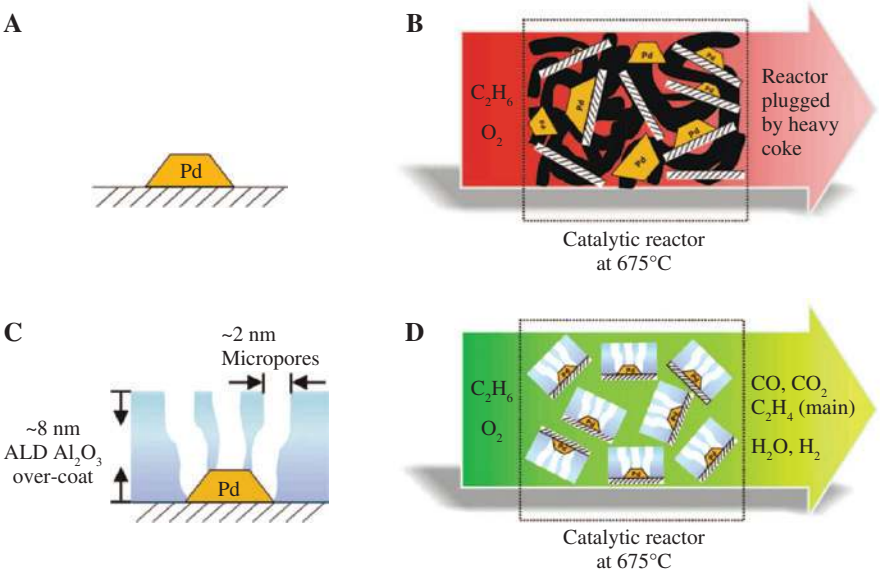

Figure 4: Schematic model of Pd/Al_2O_3 catalysts with and without an ALD Al_2O_3 overcoat during the oxidative dehydrogenation of ethane reaction at 675°C. (A) The uncoated Pd/ Al_2O_3 catalyst. (B) The uncoated Pd/ Al_2O_3 catalyst during ODHE reaction. (C) The Pd catalyst with an ~8-nm ALD Al_2O overcoat. (D) The ALD Al_2O_3-overcoated Pd/Al_2O_3 catalyst during ODHE reaction. Reprinted with permission from Ref. [26]. Copyright 2012 American Association for the Advancement of Science.

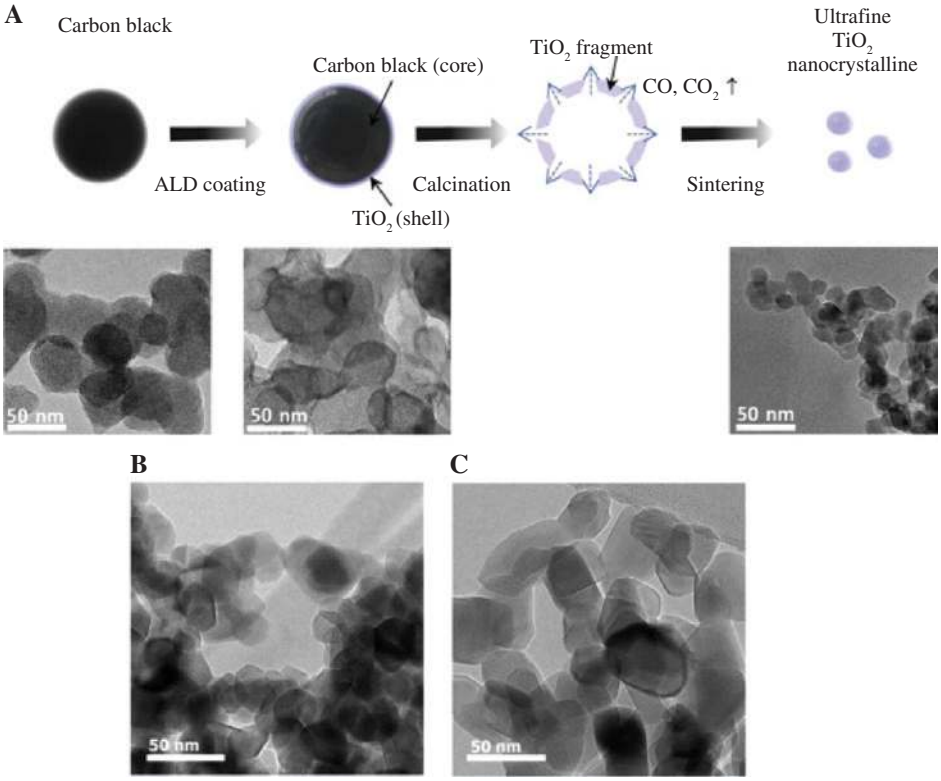

Figure 5: (A) (Top) schematic illustration of ALD assisted sacrificial template method for TiO_2 nanocrystalline anode synthesis. (Down) SEM and TEM images of the materials obtained at each processing step. HRTEM images of TiO_2 produced from the carbon black encapsulated by ALD coating layers with (B) 3- and (C) 10-nm thicknesses. Reprinted with permission from Ref. [40]. Copyright 2015 Elsevier B.V.

accomplished conformal deposition of a nanoscale-thick TiO_2 layer on a carbon black template surface and, subsequently, removed the template by thermal calcination. The calcination and subsequent sintering process generated mesoporous TiO_2 and further transformed the TiO_2 particles into spherical nanocrystallites. This mesoporous nanostructure with a large surface area exhibited a greatly enhanced reversible capacity, approaching the theoretical value. Furthermore, owing to the thermally activated catalytic effect of the TiO_2 shell, the inner carbon black template can be removed without leaving any residue at relatively low temperature. However, the pure carbon black template without an ALD coating could only be completely burned at a high temperature over 700°C.

2.2 One-dimensional nanomaterials

The 1D materials with nanoscale structures have shown a variety of applications due to the large surface-to-volume ratio and quantum confinement [44, 45] effects. One of the widely used ways to form the 1D structure is through template. Based on the template, coating the surface of a 1D template is able to confine lateral dimensions of the materials, and subsequently, hybrid and hollow structures with novel physical and chemical properties can be synthesized by etching of the core and reacting with the shell.

Direct coating on the template is the common way for the preparation of 1D nanomaterial preparation. For example, Woo et al. [46] successfully fabricated sub-5-nm nanotrenches and nanowires by transferring a CNT pattern. Borbón-Nuñez et al. [47] fabricated TiO_2 tubes by coating the multiwalled carbon nanotube (MWCNTs) surface with TiO_2 using ALD. They demonstrated that thick-walled (20 nm) TiO_2 tubes can be obtained by direct ALD TiO_2 coating, while for thinner-wall tubes (10 nm), a very thin Al_2O_3 buffer layer was inserted to enhance the structural stability of the TiO_2 tubes.

Among the 1D templates, polymer-based templates have the advantage for their being easy to remove and their flexibility when constructing various structures. Its template is often formed by electro-spinning or sputtering to maintain the nanoscale-sized templates. The surface of these densely packed polymers is often covered with highly reactive groups, and the inorganic film rapidly nucleates on the polymer surface, thus, forming a

conformal inorganic coating. Because of the 1D morphology of spun polymers, they are more applicable to 1D core-shell structures, as well as the hollow structure by etching the core of their structures, for example, the organic-inorganic core-shell nanofibers of ALD GaN on electrospun polymeric nanofibers [48] and the hollow nanotubes with tunable diameters and wall [49]. This generation of hollow nanofibers often involves three processes: electrospun polymer templates, ALD shell layer formation, and selective removal of the polymer templates, as depicted in Figure 6. Kayaci used ZnO as a model semiconductor and systematically characterized the effects of calcination on the morphology and crystallinity of ALD ZnO on nylon 6,6 nanofibers [50]. They suggested that an excessive increase in surface area cannot result in an equivalent enhancement of the photocatalytic activity, and a careful balance of the surface area and defect density is required. However, if the polymer is amorphous, and the functional groups are nonreactive, the precursors can diffuse into the polymer and react within the film, resulting in an embedded inorganic phase in the organic bulk.

As for organic materials, the template is often removed by solution dissolve or post calcination. Guan et al. [51] coated ZnO and TiO_2 on the SnO_2 nanowires by ALD, then dissolved the ZnO sacrificial layer to form a hollow and conformal TiO_2 shell. This surface-engineered method used an SnO_2 nanowire as the template and obtained a new type of hollowed SnO_2-in-TiO_2 wire-in-tube nanostructure. This structure radically improved the rate capability and cycling stability, compared to both bare SnO_2 nanowire electrodes. It can be attributed to the uniform TiO_2 shell protection, as this protection layer can simultaneously stabilize the solid electrolyte interphase layers and accommodate the volume expansion of the SnO_2 core wire. Deng et al. [45] systematically investigated the formation of porous metal oxides (Al_2O_3, TiO_2, V_2O_5, and ZnO) with different morphologies using atomic layer deposition on multi-walled carbon nanotubes followed by post deposition calcination. The morphological transformations during calcination are summarized in Figure 7. In addition, they pointed that the crystallization temperature and the surface coverage of the metal oxides and the oxidation temperature of the carbon nanotubes have significant influence on the final morphology. Lotfabad et al. [52] coated TiO_2, TiN, and Al_2O_3 ALD films on the outer or inner surfaces of hollow Si nanotubes and demonstrated that the coated composites have a positive influence on the cycling performance of Si nanotube electrodes, and they show relatively little structural damage and good cycling stability.

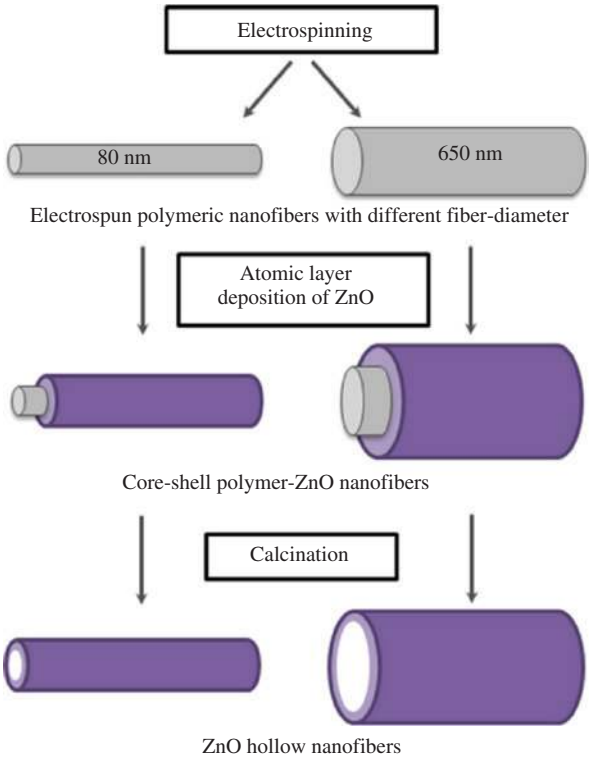

Figure 6: Schematic diagram depicting the steps involved in the production of core-shell and hollow nanofibers. Reprinted with permission from Ref. [50]. Copyright 2015 Elsevier B.V.

Except for the eliminating process combined with ALD coating for 1D nanostructure fabrication, other processes on inorganic templates are also important for 1D nanostructure fabrication. For instance, Guan et al. [53] constructed a novel hollowed wire-in-tube nanostructure of CoO-in-$CoSnO_3$ through ALD. They first obtained $Co_2(OH)_2CO_3$ nanowires by a hydrothermal method and then deposited ALD SnO_2 on it. This CoO wire-void-$CoSnO_3$ tube was formed through a proper thermal treatment, in which the $Co_2(OH)_2CO_3$ decomposed and reacted with the outer SnO_2 layer simultaneously. Because of the hollow feature of CoO-in-$CoSnO_3$, it showed much better electrochemical performance compared with the bare CoO nanowire. Jin fan et al. [54] demonstrated the fabrication of high-aspect-ratio nanotubes based on the Kirkendall effect. They transferred the ZnO-Al_2O_3 core-shell nanowires with a uniform ALD coating of the amorphous Al_2O_3 into a single-crystal $ZnAl_2O_4$ spinel nanotube through a solid-state reaction, which is based on the Kirkendall effect. The principle is that when the out-diffusion of the core material through the spinel is faster than the in-diffusion of the shell material, the Kirkendall voids generate. As the reaction is completed, it leads to hollow spinel nanotubes. The use of the Kirkendall effect allows a rational design of nanoscale hollow objects, providing another approach to the fabrication of nanotubes of a variety of materials.

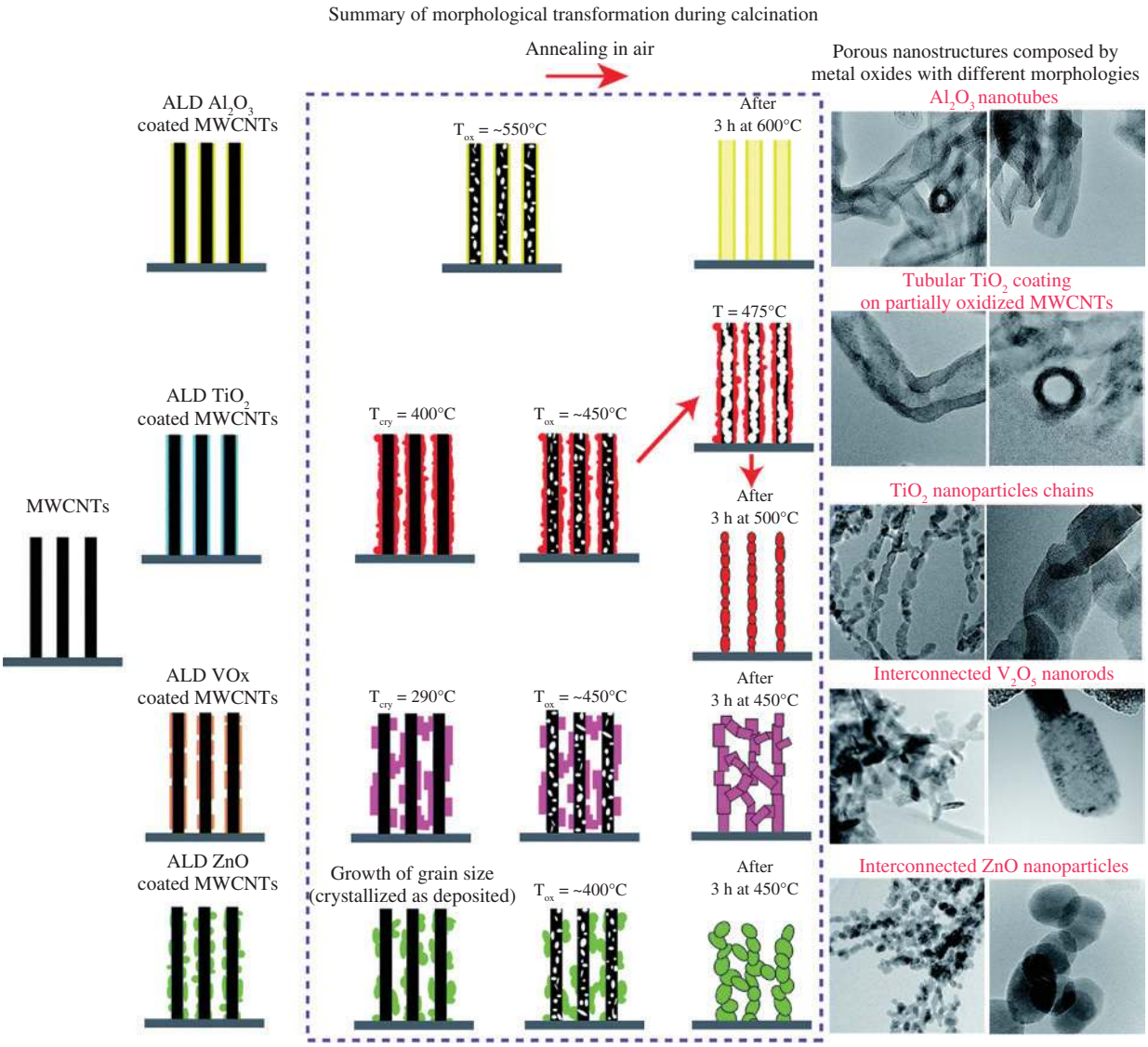

Figure 7: Schematic demonstration of the formation of porous metal oxide nanostructures by ALD on MWCNTs followed by calcination. Reprinted with permission from Ref. [45]. Copyright 2014 Royal Society of Chemistry.

2.3 Complex nanostructures

Because of the self-limiting reactions, ALD is able to grow uniform and conformal films on all coated surface in a precisely controlled way. This capability provides a straightforward way for tuning the properties of nearly any surface. In this sense, ALD is a powerful tool for the synthesis of nanostructured materials or functionalized nanostructured materials.

Replication of porous template structure is a valid way for nanostructure fabrication and has been used for surface functionalization. Anodic aluminum oxide (AAO) template has high potentials in various nanofabrication processes for its high aspect ratio and porous features. For example, Haider's group [55] grew electrochemical polycrystalline bismuth (Bi) nanowires in highly ordered porous AAO templates. They replicated the AAO template structure by ALD SiO_2 and electrochemically depositing Bi nanowires on it. Results showed that the ALD SiO_2 not only replicated the AAO structure with accurate size control (30 nm) but also acted as a protective layer on the surface of the wires. Another classical application of AAO is the nanoarray fabrication through structure replication. For example, Yao's group [44] fabricated TiO_2 nanowire arrays by replicating the AAO template (Figure 8). After the fabrication of nanoporous AAO templates, TiO_2 thin films were grown by ALD and sputtering, followed by selective removal of the aluminum substrate and AAO

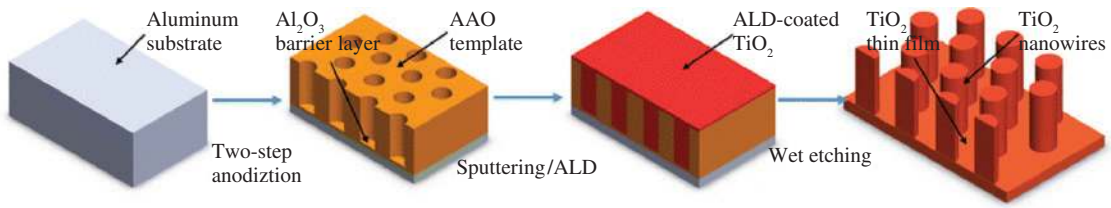

Figure 8: Schematic diagram of the processes to produce nanowire arrays. Reprinted with permission from Ref. [44]. Copyright 2015 Springer.

template via a wet etching process. Through this method, large-scale and free-standing TiO_2 nanowire arrays were formed. They also confirmed that the sputtered TiO_2 formed mushroom-like structures on the AAO template surface, while the ALD-coated TiO_2 filled the AAO holes finely, exhibiting clear crystal grain boundaries. By using diverse AAO templates, it is simple to synthesize highly ordered TiO_2 nanowire arrays with desired parameters like diameter and density.

In addition to nanowire arrays, other complex structures based on the AAO template have also been presented, e.g. the sharp-edged crescent-shaped half-nanotubes (HNTs) [56], the tube-in-tube nanostructures and multisegmented nanotubes. The process is depicted in Figure 9. By controlling the removal of the sacrificial ALD layer onto the AAO template pore walls, this method allows convenient control over the morphological properties, such as edge sharpness, gap size, and wall thickness of HNTs. Gu et al. [57] accomplished successive fabrication of tube-in-tube nanostructures by growing ALD nanotubes on the interior template walls of the AAO nanochannels. By alternate removal of Al_2O_3 sacrificial spacers to release nanotubes replicated from the AAO template, multiple-walled coaxial nanotubes of five nested layers were synthesized within AAO templates. The resultant coaxial nanotube structures are highly ordered and absolutely conformal with the template pore structure and can achieve very high aspect ratios. Bae et al. [58] further described a general strategy for fabricating multisegmented nanotubes and nanopores via sequential, surface-selective modification

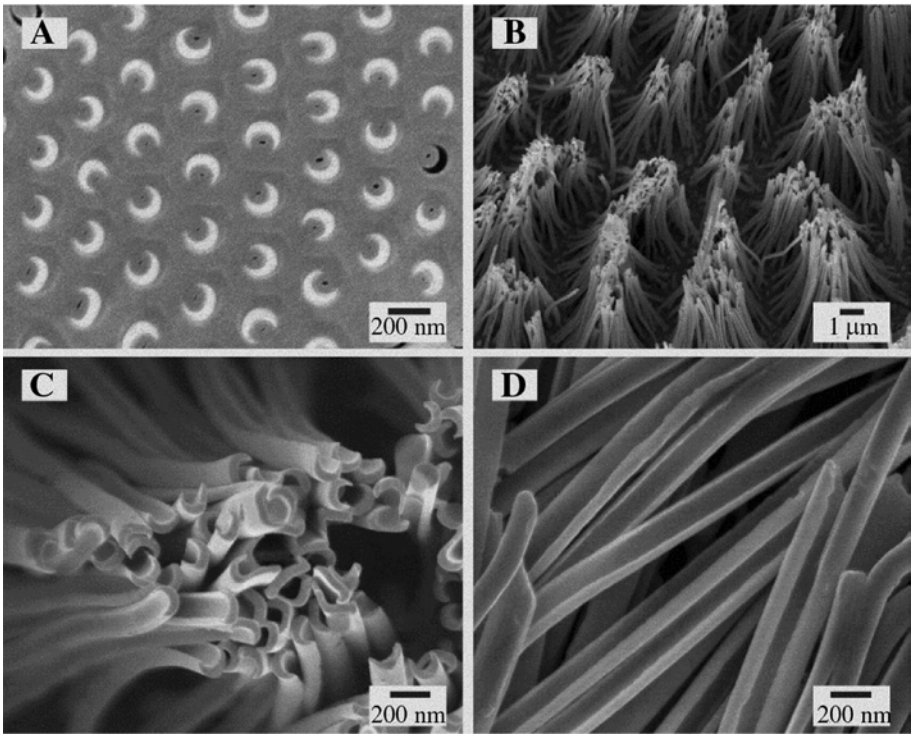

Figure 9: (A) Cross-sectional SEM image of an AAO template after electrodeposition of Au into the crescent-shaped nanochannels created with ZnO sacrificial layer. (B, C) Top-view SEM images of the HNT arrays released by dissolving the template. (D) A close-up of the HNTs. Reprinted with permission from Ref. [56]. Copyright 2011 American Chemical Society.

with organic and inorganic layers combined with *in situ* formation of nanopores by electrochemical anodization. First, the octadecyltrichlorosilane (OTS) self-assembled monolayers (SAMs) were formed on the alumina templates as the first organic segment. Subsequently, the SAM-coated pores were separated from the underlying Al when the Al foil was anodized. As the inert surfaces of methyl-terminated OTS-SAMs hinder the desired ALD reactions, the freshly grown pore section was selectively coated with an inorganic layer (TiO_2, ZnO, or ZrO_2) using ALD. In this way, the inner surfaces of nanopores can be chemically and physically modified in a segmented manner with organic/inorganic materials.

Based on the templates and ALD technology, combining with another solution growth, it is capable of constructing complex architecture. For example, Karuturi and co-workers [59] designed a new type of nanowire-inverse opal hybrid architecture involving the assembled colloidal sphere templates, the ALD TiO_2 film, the ALD ZnO seed layer, and the ZnO nanorods by standard solution growth. The process is depicted in Figure 10. The bilayer nanostructures were in intimate physical contact with high crystallinity, and the photocurrent performance of this bilayer was evidently improved. Kayaci et al. [60] explored the electrospun poly(acrylonitrile) nanofibrous as the templates, and grew the single crystalline ZnO nanoneedles with high optical quality on the ALD seeds via hydrothermal process. This novel structure showed enhanced photocatalytic activity because of the catalytic activity at surface defects (on ALD seed), valence band, and conduction band (of ZnO nanoneedles). Cheng et al. [61] fabricated the 3D hollow urchin nanowire structures by a combination of colloidal sphere self-assembly, atomic layer deposition, and subsequent hydrothermal growth. ALD TiO_2 and ZnO were deposited on self-assembled monolayer polystyrene microspheres at low temperature. The ALD TiO_2 acts as a scaffold, and the ALD ZnO layer is used as a "seed layer" for promoting ZnO nanorods growth. Because of the advantages of the mixed structure, it offers a higher surface area for quantum dot loading. Accordingly, experiments demonstrated that these 3D urchin-like structures generate a photocurrent higher than that of 2D TiO_2/ZnO inverse opals.

Except for the AAO-directed coaxial nanostructures and inverse opal, many other 3D networks have been reported in the past years, including metal foam, carbon fiber nanotube cloth, and ultrathin graphite foam (GF) [62]. For example, Guan et al. [62] directly confined Fe_2O_3 nanoparticles on 3D GF and utilized them as anode for Li-ion batteries. Because of the 3D nanostructure, this GF@Fe_2O_3 electrode demonstrated outstanding rate capability and cycling stability as the porous GF provides a stable, highly conductive support and a short ion diffusion length for fast reversible reaction. This function can further be extended to flexible carbon substrate, for instance, the NiO nanoparticles on flexible graphite foam-CNT forest substrate [63] and Co_3O_4 nanolayers on the flexible carbon nanotube/carbon cloth substrate [64]. The mechanically robust carbon-based substrate, the uniform ALD coating layers, together with the unique hierarchical structure contribute to the high areal capacitance and excellent cycling ability for supercapacitors. In addition, other porous materials with ALD coating layers are presented. Jang et al. [65] created the 3D hollow rigid lattices involved with the ALD TiN layer. The constituent solids attain tensile strengths of 1.75 GPa without failure even after multiple deformation cycles. Therefore, they suggested that the hierarchical design principles can be

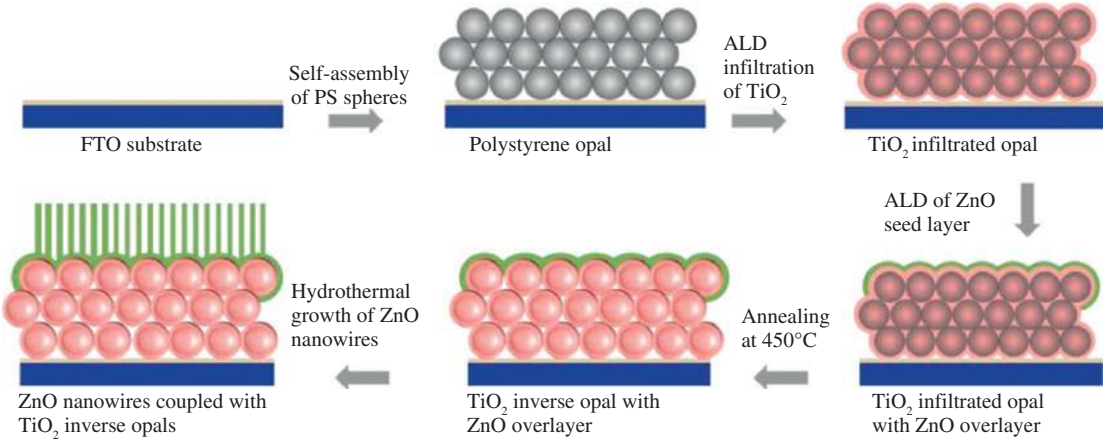

Figure 10: Schematic of the fabrication procedure of bilayer photoanodes in which TiO_2 inverse opal is coupled with ZnO nanowire arrays. Reprinted with permission from Ref. [59]. Copyright 2012 Elsevier.

applied to create damage-tolerant lightweight engineering materials. Werner et al. [66] demonstrated the applicability of atomic layer deposition for the fabrication of multifunctional ordered mesoporous core-shell nanocomposites. Their results suggest that ALD can homogenously coat 3D co-continuous gyroidal mesoporous templates with well-defined pore sizes below 50 nm and thicknesses above 10 mm. However, challenges for the deposition of nanoscale 3D surface still exist. Incomplete saturation reaction may occur when the substrate has small openings and spaces, which limits the quality of the coating layers. Well understanding the precursor-surface reactions are needed to achieve the well controlled deposition within 3D structure, including the size and volatility of precursor and the thickness and composition of the substrate. As for the experimental aspect, varying exposure time or working pressure may achieve good saturation to reach the ideal conformality [67].

3 Surface treatment

From the perspective of surface chemistry, as ALD half-reaction relies on the saturated adsorption process, the initial surface state has a significant effect on the nucleation of ALD films. Therefore, artificial manufacture of the surface, including active groups and surface defects, is a convincing approach for rational design and tuning of ALD film characteristics as the type, density of active groups, and the surface defects also determine the quality and performance of the film. Depending on the function, i.e. enhancement or prevention of the reaction, surface treatments are divided into two types: surface activation and surface blocking.

3.1 Surface activation

According to the growth mechanism, the ALD nucleation reaction only occurs at surface-active sites and defects. However, native sites are often not reactive enough to modify the desired reaction. For example, coatings on sp^2 carbon materials suffer non-coating or incomplete coating [68] due to the lack of dangling bonds for adsorption. It is shown that ALD reactions only occur at the step edges [69, 70] and surface defects [71] of pristine carbon materials, which form nanoparticles or nanowires. Therefore, surface activation is proposed as a method for creating or increasing the density of active sites and defects to promote nucleation.

Surface activation can carry out directly and indirectly. The direct surface activation often involves chemical covalent surface treatments, which manipulate the nucleation sites to increase and homogenize the growth of a film. This surface engineering aims at increasing the nucleation sites and defects, and it is a straightforward way to promote film deposition and help to transform the growth mode. For example, it has been demonstrated that the growth mode of the film can be controlled from selective decoration up to full coating, simply by controlling the degree of surface-defect engineering in the CNTs [72]. Zhu et al. [73] found that the rate of nucleation of Al_2O_3 is correlated with the amount of oxygen. They oxidized the black phosphorus samples by ambient air to modify the phosphorus oxide concentrations and found that this surface pretreatment promoted the Al_2O_3 nucleation and the uniform film growth. After the formation of phosphorus oxide, the surface reactivity changed, and the defects increased, which is helpful for Al_2O_3 nucleation. In addition, the authors also suggested that adventitious contamination of the surface could enhance the nucleation of Al_2O_3. This oxidized method works by decreasing the chemical inertness of a substrate [74] and creating new oxygen-incorporated nucleation sites [75, 76]. The oxidants include the mineral acids and the strong oxidants such as O_3 [77] and O_2 plasma [78]. Meng et al. [79] chemically functionalized CNTs prior to ALD-Fe_2O_3 by HNO_3, and the surface reactivity of CNTs is significantly enhanced. However, the as-deposited Fe_2O_3 was random and non-uniform, while the incorporation of N atoms in CNTs induces the deposition of uniform ALD-Fe_2O_3.

Although the chemical covalent functionalization method provides a powerful way to enhance the surface activity, it has some limitations, for example, the deterioration of electrical and structural properties of the pristine nanotubes and graphene. Thus, non-destructive functionalization methods are preferable. This indirect functionalization method is mainly based on supramolecular complexation [72], and it belongs to the class of second-hand surface pretreatments. By using various adsorptive and anchoring forces, precursor adsorption on the substrate is enhanced. One example is the use of hydrogen bonding, through which the precursor is physically adsorbed on the sp^2 carbon substrate. This creates nucleation sites for the latter reaction, even when the deposition temperature is relatively low. Zheng and co-workers [80] grew Al_2O_3-doped HfO_2 films on graphene by H_2O-based atomic layer deposition. Their results showed that predosing graphene with water increased the concentration of nucleation sites and introduced no defects. The dielectric film could act as a seed-like layer for the following film

growth at 200°C. Moreover, Al_2O_3-doping could act as a network modifier to maintain the amorphous structure of Al_2O_3-based HfO_2 stacks on graphene, even at 800°C. Besides the hydrogen bonding, other forces such as van der Waals and π-π interactions, are also helpful for reinforcing the bonding between the surface and precursor. For instance, through nondestructive π-π stacking of a reactive molecule (4-mercaptophenol) on a graphene surface, Han et al. [81] obtained uniform and conformal ZnO thin films on graphene, which have good quality with a low density of pinholes.

It is reported that ALD deposition occurs preferentially in areas where the material has already been deposited in preceding cycles [72]. Therefore, the ALD seeding layer is of considerable importance to thin-film formation. The seed layer can even provide a non-destructive way to determine the overall properties of the resulting film [82]. Farmer and Gordon [83] found that trimethylaluminum (TMA) reacts with NO_2, forming a stable complex on the single-walled carbon nanotube (SWNT) surface at room temperature. After the completion of the 50 cycles of NO_2-TMA functionalization and 5 cycles of Al_2O_3 ALD stabilization steps, the structure can be used as a scaffold for growing many other materials by ALD. Young and co-workers [84] confirmed that Al_2O_3 islands produced by NO_2/TMA pretreatment help to increase the density of nucleation sites and facilitate the onset of Al_2O_3 growth. Furthermore, the Al_2O_3 films grown after the NO_2/TMA pretreatment also showed a reduced thickness and better resistance. Bielinski and co-workers [85] showed that ALD is a reliable surface modification method to guide nanowire orientation. They grew hierarchical ZnO nanowires by ALD seeding. The seed layer was used to promote heterogeneous nucleation of the nanowires. By simply varying the cycles of ALD ZnO, the morphology of hydrothermally grown ZnO nanowires could be tuned reliably. They concluded that the texture of the seed layer influenced the orientation of the resulting nanowires.

3.2 Surface blocking

In contrast to surface activation with the aim of promoting surface reactions, surface blocking is designed to block the surface site areas selectively. The selective process is unique in that no etching steps are needed for selective deposition. From the perspective of basic principle, the key for achieving this blocking is to weaken the dissociative chemisorption of co-reactant molecules on substrate surface. On this basis, several strategies are adopted. One is to adjust the ALD process parameters, such as the temperature, pressure, and substrate materials [30]. Weber et al. [86] reported a novel strategy for synthesizing Pd/Pt core/shell nanoparticles supported on Al_2O_3 substrates. As the dissociative chemisorption of O_2 only takes place on the platinum group metals but not on oxide support material, they achieved selective deposition of Pt only on the surface of Pd. Furthermore, they found that the shell growth takes place only when the size of the Pd core is larger than 1 nm. Their results clearly demonstrated that ALD enables precise and independent control of the core and shell sizes of bimetallic core/shell NPs. Lu et al. [87] explored a variety of deposition temperatures, co-reactants, and pulse-sequencing strategies to achieve the desired selectivity. They synthesized supported bimetallic nanoparticles by properly selecting the deposition temperature and the appropriate co-reactant. The second metal only deposited on the surface of the first metal, while the monometallic nanoparticle formation is avoided. Meanwhile, the size, composition, and structure of the bimetallic nanoparticles were precisely controlled by tailoring the precursor pulse sequence.

Unlike controlling the ALD process parameters, Yanguas-Gil et al. [88] proposed a different surface-functionalization step to control the dopant distribution and achieve higher doping efficiencies. By adding ethanol (EtOH) to the conventional precursor/coreactant ALD sequence, they reduced the density of surface reactive sites and, therefore, effectively achieved controlled, submonolayer saturation coverage. As EtOH displaces surface hydroxyls and blocks potential adsorption sites for the TMA, the growth of Al_2O_3 was inhibited, but they are removed during the H_2O exposures, allowing the Al_2O_3 ALD to proceed. When used to deposit Al-doped ZnO, this functionalization/precursor/coreactant sequence ALD films exhibited carrier concentrations two times higher, on average, than conventional ALD films of similar Al concentration.

However, the main stream to achieve area selectivity is to use the spatially controlled blocking resist [89]. According to the molecular weight, the selective strategy can be divided into processes involved with molecular blocking agents and self-assembled monolayers (SAMs). The molecular blocking agent originates from the large molecular groups or generated by-products. These bound groups are chemically inert to precursors that occupy the active sites of the substrate and prevent the subsequent adsorption process. In the study of the formation of copper nanoparticles on zinc oxide powder [90], results showed that when the surface runs out of available hydrogen, the remained hexafluoroacetylacetonate ligands hinder continuous copper film formation. In addition, novel nanostructures can be fabricated with the blocking agent. For instance,

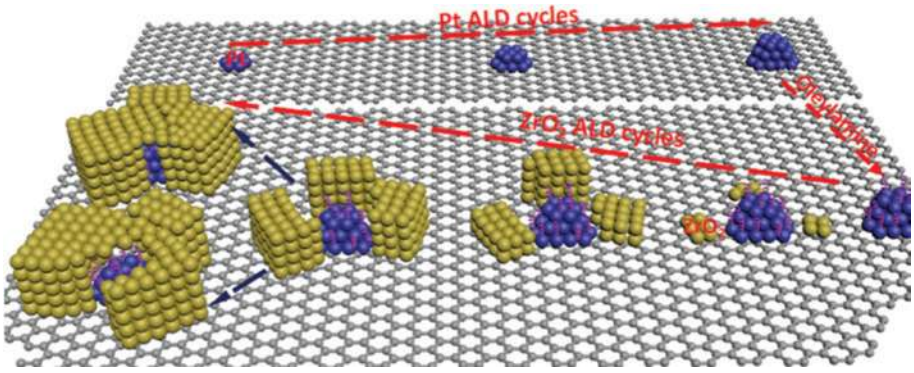

Figure 11: Schematic diagram of zirconia-encapsulated platinum nanocage structure fabricated by area-selective ALD. Reprinted with permission from Ref. [93]. Copyright 2014 John Wiley and Sons.

Ray and co-workers [91] developed a strategy to synthesize nanobowls by utilizing this blocking effect. This method involves the growth of uniform and dispersed ALD Pd nanoparticles, blocking agent for protecting the particles, the use of ALD in the formation of metal oxide structure around the nanoparticle, and the removal of blocking agent. This nanobowl is very advantageous in catalysis [92] because the unique, feathered structure imparts high catalytic activity and facilitates simultaneous separation of reactants and catalysts. Cheng et al. [93] designed a novel structure to stabilize Pt catalysts by area-selective ALD. They formed a nanocage structure (Figure 11) by selectively growing ALD zirconia around the Pt NPs. The Pt NPs were initially deposited on nitrogen-doped carbon nanotube (NCNT) by ALD, followed by the application of a blocking agent (oleylamine) to the Pt NP surface. The ALD zirconia was not deposited on the Pt surface due to the blocking agent. As the zirconia nanocages prevented the migration and agglomeration of Pt NPs on the support, the Pt NPs encapsulated in a zirconia nanocage show nine and 10 times more stability than ALD Pt/NCNT and Pt/C catalysts, respectively. Additionally, this catalyst exhibited an oxygen reduction reaction (ORR) activity 1.4 and 6.4 times greater than that of ALD Pt/NCNT and Pt/C, respectively, due to the small-size Pt NPs and the synergetic effects of Pt and ZrO_2.

In addition to the molecular blocking agents, SAMs are the common blocking agents used for area-selective deposition. With SAMs, area-selective ALD greatly expands the applicability of ALD for fabricating novel structures and can be readily applied to the growth of other compositions. Generally speaking, SAMs consist of the following three parts: a long organic molecule backbone, head, and tail groups. SAMs offer a way to achieve area-selective ALD by alternating the appropriate tail group to block ALD precursors from attaching to the surface. For instance, through the deposition of octadecyltrichlorosilane (ODTS), the SiO_2 substrate was changed from hydrophilic to hydrophobic with the replacement of -CH_3 to -OH to cover the substrate [94]. Generally, SAMs are hydrophobic and serve as a layer to inhibit nucleation. For example, Cao and coworkers [94] utilized the commonly used ODTS SAMs to modify the surface. As the active sites were occupied by SAMs, the pinholes on the SAMs were used as active sites for the initial core nucleation. Subsequently, the second metal was selectively deposited as the shell layer. In the second stage of deposition, as the nucleation sites can be effectively blocked by surface ODTS SAMs, Pd/Pt and Pt/Pd NPs with uniform core-shell structures and a narrow size distribution were successfully formed. As both processes were conducted by ALD, sample transfer was avoided, and independent engineering of the dimensions of the catalyst can be easily achieved.

Except for the nucleation-inhibition layer for 0D coatings, SAMs can be utilized to grow planar or even more complex structures. For instance, Minaye Hashemi et al. [95] employed a strategy to selectively deposit films on Cu/SiO_2 substrates, as shown in Figure 12A. By using the intrinsically selective adsorption of octadecylphosphonic acid SAMs on Cu over SiO_2 surfaces, they selectively patterned a resist layer only on the Cu surface. Then, they applied ALD Al_2O_3 on the patterned surface and removed any residual dielectric film deposited on the Cu surface, leaving the dielectric Al_2O_3 film on SiO_2 unaffected. Moreover, it greatly expanded the thickness limits of selective deposition of dielectric materials on a metal/dielectric pattern, with an increase from 6 nm to 60 nm. However, things changed when ALD was applied to the non-planar surfaces. Chopra et al. [96] found that SAMs formed defects in the high curvature region, allowing nucleation of ALD TiN films. This is in contrast to the SAM covering planar surface, which exhibits a complete blocking TiN film. Similar to Minaye Hashemi et al. [95], Dong et al.

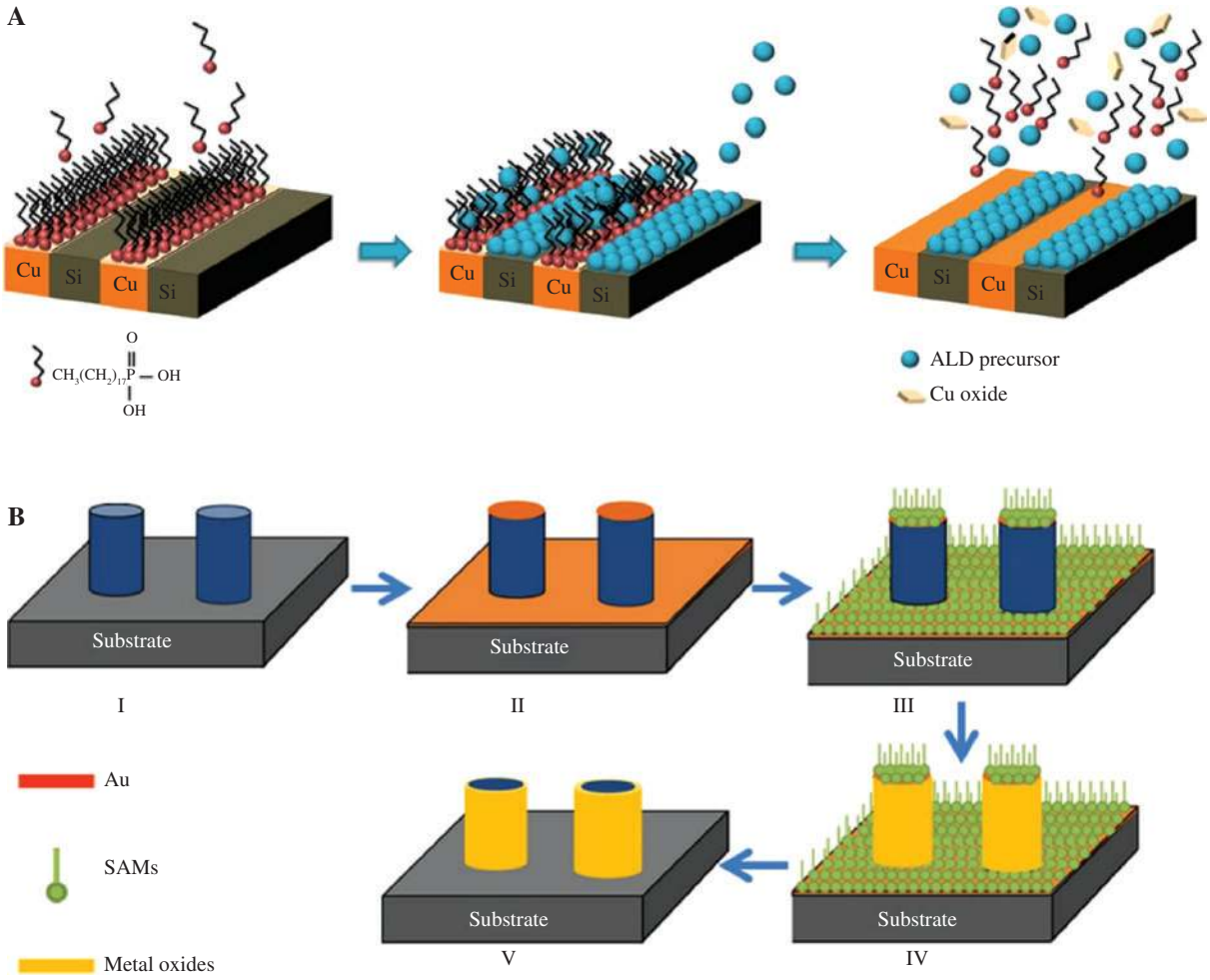

Figure 12: (A) Schematic demonstration of self-aligned patterning through a combination of selective deposition and selective removal of dielectric material. Reprinted with permission from Ref. [95]. Copyright 2015 American Chemical Society. (B) Schematic diagrams of the 3D (area-selective) ALD of a metal oxide on the vertical surfaces of standing nanopillar structures. Reprinted with permission from Ref. [97]. Copyright 2014 Nature Publishing Group.

[97] achieved the selective coating of the vertical surfaces of standing nanopillars. By utilizing the hydrophobic SAMs, they selectively inhibited the ALD ZnO coating on the modified horizontal regions, ensuring that only the vertical surfaces of the vertical standing nanorods were coated, as depicted in Figure 12B. These results further confirmed that ALD is a feasible process by artfully exploiting hydrophobic SAMs to tune the area-selective formation of ALD films on the horizontal and vertical surfaces of substrates.

Direct patterning the SAMs presents another effective way for area-selective ALD as the morphology of the patterned films depends on the SAM structures. This direct manufacturing on SAMs can be accomplished through various means such as microcontact, energetic beams, and so on. For instance, Färm et al. [98] prepared patterned SAMs using an elastomeric stamp, which transferred the patterned SAMs to the surface within just seconds. This fast microcontact printing process eliminates the need for a separate patterning process. They verified the passivation properties of the printed SAMs of iridium and TiO_2 grown by ALD processes and found the SAMs to be a well-patterned mask layer, with film growth occurring only in the non-SAM areas. Hua et al. [99] achieved pattern definition by thermal-probe-based lithography strategies. They utilized heated cantilever probes to locally decompose the polymer film, which served as a template for subsequent ALD growth, resulting in line patterns to obtain nanowire structures. In addition to rational utilization of their properties, SAMs can aid the construction of nanostructures. Huang and co-workers [100] applied the electron-beam to the previous self-assembled ODTS, then, selectively grew ALD films on places that are not covered with OTDS. With SAMs, area-selective ALD greatly extends the applicability

of ALD for fabricating novel structures and can be readily applied to the growth of complex compositions.

However, challenges still exist as the SAMs are sensitive to high temperature and degrade over time. For example, if the exposure time is long enough, the ODTS will degrade. Therefore, decreasing the ALD film deposition temperature while maintaining the film qualities is of great importance [89]. For example, the good-quality Al_2O_3 thin films were prepared on polyethylene naphthalate substrates at 35°C without damaging the substrate [101], and the compact ALD TiO_2 layers were fabricated on perovskite solar cells with a power conversion efficiencies as high as 11.2%. Therefore, the growth of high-quality thin films at low temperature is very attractive for heat-sensitive films [102].

4 Enhanced atomic layer deposition

Film coating by ALD still faces some challenges in addition to the strategies mentioned above. For example, insufficient activity of the precursor leads to undesirable structures in the obtained films. Therefore, additional enhanced strategies on ALD are expected to counter these challenges.

4.1 Reactor extension and redesign

4.1.1 Plasma

In the case of thermal ALD, it is possible to coat various films by surface modification strategies. However, some precursors need more energy to activate their chemical reactions, while the introduction of plasma is a good solution. Compared to thermal ALD, the introduced plasma offers greater freedom for the choice of processing conditions and the available precursors [103]. ALD with plasma is generally called plasma-enhanced atomic layer deposition (PEALD) [104].

One of the greatest advantages of PEALD is that plasma can help to decrease the deposition temperature [105], which is beneficial for the process in many respects. For example, due to the energy provided by H_2-plasma, the deposition can be conducted at low temperatures. Minjauw and co-workers [106] deposited Ru thin films at 50°C, while the general thermal ALD process for Ru thin films must be conducted at 100°C. This near-room-temperature deposition may be attempted on polymers, without degradation during the experiment. As the low deposition temperature by plasma extends the ALD temperature window, PEALD is likely to enable completely new processes that are not accessible by thermal ALD [107]. For example, Griffiths et al. [31] reported the first gold metal deposition by ALD with oxygen plasma, while other oxygen-containing coreactants (e.g. H_2O and O_3) were unreactive with the trimethylphosphinotrimethyl gold(III) precursor under thermal conditions. Schindler et al. [108] demonstrated the deposition of PEALD $BaTiO_3$ for the first time using cyclopentadienyl(Cp*)-type barium precursor. Their results showed that PEALD can produce denser and more uniform $BaTiO_3$ films, compared to thermal ALD $BaTiO_3$.

Furthermore, experiments showed that PEALD films are likely to have less contamination and improved film quality [109]. The extra energy offered by plasma is helpful for removing surface contaminants and increasing the local temperature to induce transformation of the amorphous film into the crystalline state because surface contaminants are considered to hinder the crystallization of the film. For instance, Assaud et al. [105] presented that the roughness of thermally grown TiN layers is higher than those formed by plasma-enhanced ALD, and so as the film resistivity. Musschoot et al. [110] found that V_2O_5 can transform from the amorphous state to 001-oriented crystallinity at 150°C when oxygen plasma was used as an oxidizing agent instead of water. This difference may contribute to the formation of a high-purity film because the other films have a significant amount of carbon contamination. They confirmed that the PEALD reactions lead to a higher growth rate. As the PEALD reaction saturates much faster than that in thermal ALD, a growth rate of approximately 0.7 Å/cycle was achieved during PEALD. All in all, PEALD brings many advantages to film coating. However, the plasma processing can also be compromised by reduced film conformality and substantial substrate damage, which should be noted in the process [105].

4.1.2 Fluid bed reactor

The novel chemical and mechanical properties of nanoparticles are of interest, but their high surface energy limits their applications. Coating particle surface by ALD has proven to be an effective way to maintain their unique properties. However, due to the difficulty of precursor infiltration, the general ALD process does not result in uniform coating of the unsupported particle surface. Changing the reactor design by adding the fluid bed reactors (FBRs) is expected to address this problem. With FBRs, ALD can directly modify the particle surface while

retaining its properties. The fluidized bed reactor has many advantages, including good mixing, large gas solid contact area, high efficiency for mass and heat transfer, and large-batch processing capability. By rigorous mixing of the nanoparticles through suspension and vibration, FBRs transform nanoparticles into a fluid-like state. This intimate contact improves the vapor solid contact efficiency and the heat transfer coefficients, and reduces particle aggregation. Moreover, the operation increases the precursor residence time, thus, dramatically improving the precursor utilization from 78% to nearly 100% [111]. A comparison of conventional ALD and FBR-ALD is illustrated in Figure 13 [112].

The assistance of FBR is essential for fabricating ALD thin films on core-shell nanoparticles, without the use of SAMs and templates [113]. Such a conformal and uniform film on fine particles is exemplified in Figure 14. The uniform, amorphous, and conformal iron oxide layers cover the entire surface of individual zirconia nanoparticles in the fluidized bed reactor. The excellent thickness performance, achieved through the violent mixing process, is especially suitable for functionalizing particle surfaces. For example, experiments have shown that dense and uniform nanoscale Al_2O_3 passivation layers can effectively protect Fe_3O_4 nanoparticles from oxidation, preserving their magnetic properties [111]. With this functional layer,

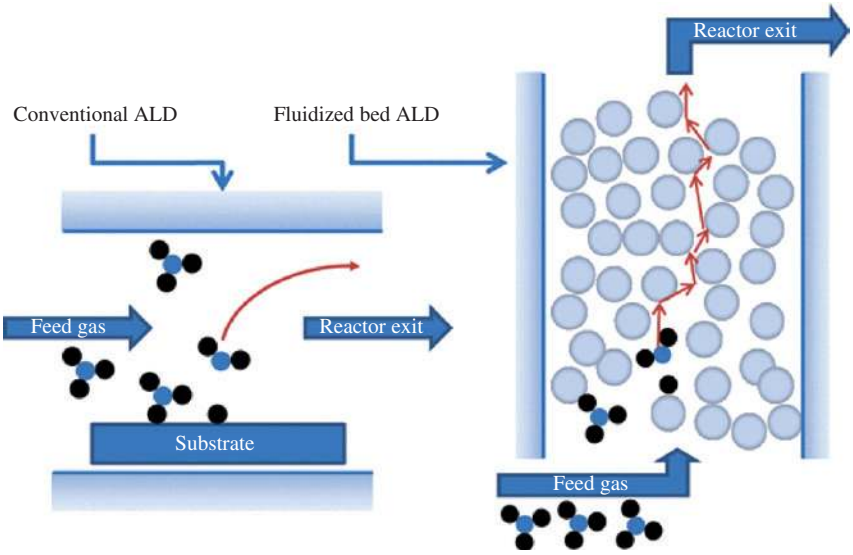

Figure 13: Removal of molecules in a "conventional" ALD reactor with a single substrate and a fluidized bed ALD reactor filled with particles. Reprinted with permission from Ref. [112]. Copyright 2016 Springer.

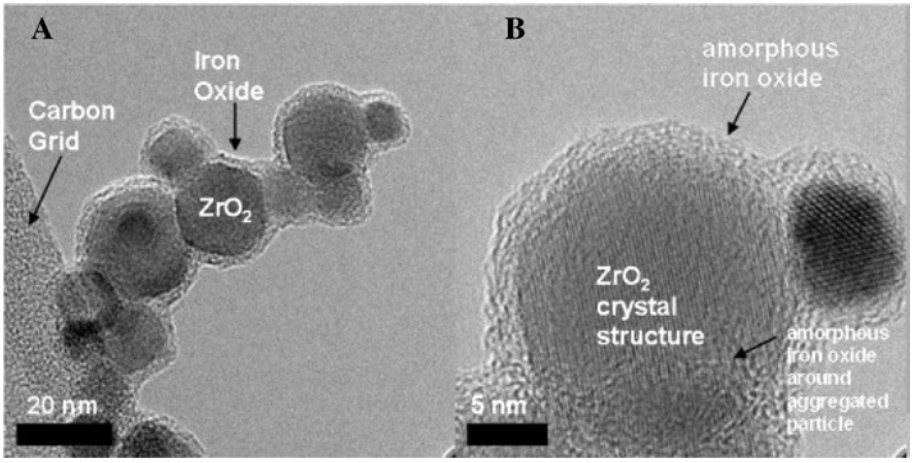

Figure 14: HRTEM micrographs of iron oxide layers on zirconia nanoparticles. Reprinted with permission from Ref. [114]. Copyright 2008 Elsevier B.V.

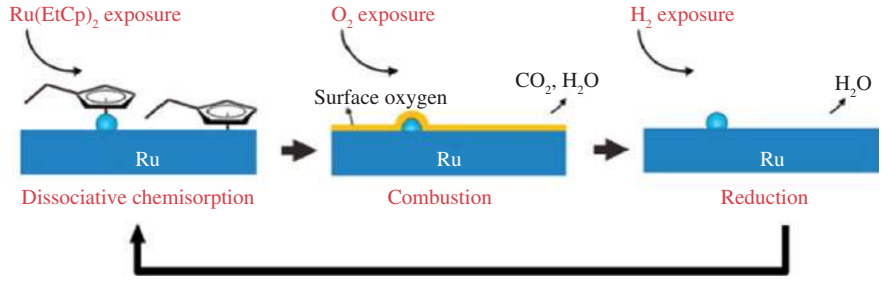

Figure 15: Schematic model of ABC-type Ru ALD, using the sequence $Ru(EtCp)_2$-O_2-H_2 on a Ru metal surface. Reprinted with permission from Ref. [119]. Copyright 2015 American Chemical Society.

this encapsulation strategy of FBRs is particularly appealing for improving the applications and performances of catalysts that require a resistance to thermal oxidation.

4.2 Improved growth model

As changing the design of the reactor helps to promote the deposition process, modifications to conventional ALD growth model present new insights into film deposition and direct new ways for film coating. For binary films, the ALD process generally involves alternating purges of two precursors into the reaction chamber. The addition of another step to the growth model, namely, the ABC-type ALD becomes prevalent in several respects, such as control over particle size, further reducing and oxidizing of the species and the additional element to the film, etc. [115]. It must be noted that in the AB-type ALD, the particle size is controlled by the number of ALD cycles, while the ABC-type ALD has the capability to control the density of the nanoparticles within an extremely narrow size distribution. Masango and co-workers [116] verified that the ALD Ag from the ABC type maintained the particle size when increasing metal loading, while the ALD Ag from the AB type formed larger particles. In addition to the controlled particle size, the ABC-type ALD yields smoother and more continuous films at the same temperature. Griffiths et al. [31] reported the deposition of Au films using the AB-type ALD and ABC-type ALD, both at 120°C. With the additional H_2O purge step at this temperature, the ABC-type ALD process accelerates the transformation of gold oxide to gold and reduces film impurities by reacting with phosphate to form the volatile phosphoric acid. Kalutarage et al. [117] showed that the growth rate of a copper film is faster for the ABC-type ALD. As the three-step process can create nucleation sites on the surface, it does not even require Cu seed layers to promote the nucleation of Cu.

In addition, the ABC-type ALD can contribute to the low-temperature process as the growth of high-quality thin films at low temperatures generally involves the inactive reactive precursor, requiring plasma and other assisted means to lower the reaction energy. For example, at a low reaction temperature, O_2 will not react (or will react incompletely) in the AB-type ALD [118], but can do in the ABC-type ALD [115] as it changes the common ALD mechanism from ligand exchange to combustion and reduction. Lu and Elam [119] achieved ALD of Ru at a temperature as low as 150°, whereas the thermal ALD of noble metals is frequently performed at a relatively high temperature of 300°C. This ABC-type ALD sequence proceeds via dissociative chemisorption, combustion, and reduction for the $Ru(EtCp)_2$, O_2, and H_2 steps, respectively (Figure 15). This $O_2 + H_2$ process is especially suitable for transforming the film from metal oxide to metal, for example, the formation of Ir [120] and Pt [121]. In general, the low-temperature ABC-type ALD involves a metal precursor, a strong acid, and an optional reducing reagent for metal ions. Metal ions in this category include silver, gold, palladium, platinum, rhodium, iridium, rhenium, tungsten, and others [122]. Except for the traditional reducing agents such as H_2, reagent combinations that release electrons during oxidative decomposition should also be included [123].

5 Conclusions

Atomic layer deposition has emerged as a valuable and effective technology in the last years. The unique features of good shape uniformity and accurate control of film thickness make ALD an enabling technology especially at addressing the negative effects when the size of material is reduced to nanometer. As shown in this review, considerable progress has been achieved with appropriate coating

strategies for ALD-based nanostructured materials in the past few years, including template-assisted preparation of low-dimensional nanomaterials and complex nanostructures, surface activation, and surface blocking treatments, and enhanced atomic layer deposition method by reactor extension and redesign or by improved growth method. With these coating strategies of ALD in mind, ALD is able to synthesize and modify materials used in many fields, for example, the core-shell nanowires for solar energy conversion [124], the synthesis of lithium ion battery components covering anodes, cathodes, inorganic solid electrolytes, the modifying of Li-ion battery with ultrathin coating layers [25], the complementary metal-oxide-semiconductor [125] and field-effect transistor [126] semiconductor device fabrication and so on.

Although with wide applications of ALD in the present time and future, ALD still faces challenges. For instance, the highly toxic H_2S [127] and expensive Pt metal precursors [128] limited the direct film deposition, as an effective precursor is a prerequisite and the key to the success of ALD. Also, the growth of heat-sensitive thin films of high quality at low temperature is still a challenge for the coating with the ALD technique, as the lack of insufficient activity of precursors leads to the failure of deposition at reduced temperatures, which is critical for heat-sensitive substrates [101]. Therefore, exploring novel precursors and better understanding of the surface chemistry and local kinetic by various in-site technologies are very important for ALD deposition. Moreover, because of the self-limiting nature, ALD is sensitive to growth environment and shows a relatively slow growth rate. Therefore, efforts devoted in atmospheric environment ALD [129] and spatial ALD [130] to achieve high deposition efficiency without sacrificing the quality of the deposition film are of increasing interest. In sum, the research on coating strategies for ALD contributes to the fabrication of novel nanostructured materials, and continuous efforts should be devoted to further promote the application of ALD.

Acknowledgments: This work was supported by the National Nature Science Foundation of China (Grant No. 21373273).

References

[1] Leskelä M, Ritala M. Atomic layer deposition (ALD): from precursors to thin film structures. *Thin Solid Films* 2002, 409, 138–146.

[2] Mackus A, Bol A, Kessels W. The use of atomic layer deposition in advanced nanopatterning. *Nanoscale* 2014, 6, 10941–10960.

[3] Soumglaude A, Tian L, Blanquet E, Brizé V, Cagnon L, Giusti G, Salhi R, Daniele S, Ternon C, Bellet D. Atomic layer deposition of TiO_2 ultrathin films on 3D substrates for energy applications. *MRS Online Proc. Libr.* 2012, 1439, 63–68.

[4] Ahvenniemi E, Akbashev AR, Ali S, Bechelany M, Berdova M, Boyadjiev S, Cameron DC, Chen R, Chubarov M, Cremers V. Recommended reading list of early publications on atomic layer deposition – Outcome of the "Virtual Project on the History of ALD". *J. Vac. Sci. Technol. A* 2017, 35, 010801.

[5] Suntola T, Antson J. Method for producing compound thin films: US, US4058430[P]. 1977.

[6] Knez M, Nielsch K, Niinistö L. Synthesis and surface engineering of complex nanostructures by atomic layer deposition. *Adv Mater.* 2007, 19, 3425–3438.

[7] Miikkulainen V, Leskelä M, Ritala M, Puurunen RL. Crystallinity of inorganic films grown by atomic layer deposition: overview and general trends. *J. Appl. Phys.* 2013, 113, 021301.

[8] Jones AC. Chemical vapour deposition precursors, processes and applications. *Kidney Int.* 2009, 56, 738–746.

[9] Parsons GN, George SM, Knez M. Progress and future directions for atomic layer deposition and ALD-based chemistry. *MRS Bull.* 2011, 36, 865–871.

[10] Crutchley RJ. CVD and ALD precursor design and application. *Coord. Chem. Rev.* 2013, 23, 3153.

[11] Ramos KB, Saly MJ, Chabal YJ. Precursor design and reaction mechanisms for the atomic layer deposition of metal films. *Coord. Chem. Rev.* 2013, 257, 3271–3281.

[12] Ozgit-Akgun C, Goldenberg E, Okyay A, Biyikli N. Hollow cathode plasma-assisted atomic layer deposition of crystalline AlN, GaN and AlxGa1-xN thin films at low temperatures. *J. Mater. Chem. C* 2014, 2, 2123–2136.

[13] George SM. Atomic layer deposition: an overview. *Chem. Rev.* 2010, 110, 111–131.

[14] Knisley TJ, Kalutarage LC, Winter CH. Precursors and chemistry for the atomic layer deposition of metallic first row transition metal films. *Coord. Chem. Rev.* 2013, 257, 3222–3231.

[15] Puurunen RL. Growth per cycle in atomic layer deposition: real application examples of a theoretical model. *Chem. Vapor Depos.* 2003, 9, 327–332.

[16] Groner MD, Fabreguette FH, Elam JW, George SM. Low-temperature Al_2O_3 atomic layer deposition. *Chem. Mater.* 2004, 16, 639–645.

[17] Gregorczyk K, Knez M. Hybrid nanomaterials through molecular and atomic layer deposition: top down, bottom up, and in-between approaches to new materials. *Prog. Mater. Sci.* 2016, 75, 1–37.

[18] Leskelae M, Ritala M. Atomic layer deposition chemistry: recent developments and future challenges. *Angew. Chem. Int. Ed.* 2003, 42, 5548–5554.

[19] Lao SX, Martin RM, Chang JP. Plasma enhanced atomic layer deposition of HfO_2 and ZrO_2 high-k thin films. *J. Vac. Sci. Technol.* A. 2005, 23, 488–496.

[20] Endo K, Tatsumi T. Metal organic atomic layer deposition of high-k gate dielectrics using plasma oxidation. *Jpn. J. Appl Phys.* 2003, 42, 685–687.

[21] Neill BJO, Jackson DHK, Lee J, Canlas CG, Stair PC, Marshall CL, Elam JW, Kuech TF, Dumesic JA, Huber GW. Catalyst design with atomic layer deposition. *ACS Catal.* 2015, 5, 1804–1825.

[22] Niu W, Li X, Karuturi SK, Fam DW, Fan H, Shrestha S, Wong LH, Tok AIY. Applications of atomic layer deposition in solar cells. *Nanotechnology* 2015, 26, 64001.
[23] Chang CY, Lee KT, Huang WK, Siao HY, Chang YC. High-performance, air-stable, low-temperature processed semitransparent perovskite solar cells enabled by atomic layer deposition. *Chem. Mater.* 2015, 27, 5122–5130.
[24] Wang T, Luo Z, Li C, Gong J. Controllable fabrication of nanostructured materials for photoelectrochemical water splitting atomic layer deposition. *Chem. Soc. Rev.* 2014, 43, 7469–7484.
[25] Meng X, Yang X-Q, Sun X. Emerging applications of atomic layer deposition for lithium-ion battery studies. *Adv. Mater.* 2012, 24, 3589–3615.
[26] Lu J, Fu B, Kung MC, Xiao G, Elam JW, Kung HH, Stair PC. Coking- and sintering-resistant palladium catalysts achieved through atomic layer deposition. *Science* 2012, 335, 1205–1208.
[27] Wise AM, Ban C, Weker JN, Misra S, Cavanagh AS, Wu Z, Li Z, Whittingham MS, Xu K, George SM. Effect of Al_2O_3 coating on stabilizing $LiNi_{0.4}Mn_{0.4}Co_{0.2}O_2$ cathodes. *Chem. Mater.* 2015, 27, 6146–6154.
[28] Kazyak E, Wood KN, Dasgupta NP. Improved cycle life and stability of lithium metal anodes through ultrathin atomic layer deposition surface treatments. *Chem. Mater.* 2015, 27, 6457–6462.
[29] O'Neill BJ, Jackson DHK, Lee J, Canlas C, Stair PC, Marshall CL, Elam JW, Kuech TF, Dumesic JA, Huber GW. Catalyst design with atomic layer deposition. *ACS Catal.* 2015, 5, 1804–1825.
[30] Lu J, Elam JW, Stair PC. Atomic layer deposition – sequential self-limiting surface reactions for advanced catalyst "bottom-up" synthesis. *Surf. Sci. Rep.* 2016, 71, 410–472.
[31] Griffiths MBE, Pallister PJ, Mandia DJ, Barry ST. Atomic layer deposition of gold metal. *Chem. Mater.* 2015, 28, 44–46.
[32] Fang GY, Xu LN, Cao YQ, Li AD. Theoretical design and computational screening of precursors for atomic layer deposition. *Coord. Chem Rev.* 2016, 322, 94–103.
[33] Ma L, Nuwayhid RB, Wu TP, Lei Y, Amine K, Lu J. Atomic layer deposition for lithium-based batteries. *Adv. Mater. Interfaces* 2016, 3, 1600564.
[34] Gougousi T. Atomic layer deposition of high-k dielectrics on III-V semiconductor surfaces. *Prog. Cryst. Growth Charct. Mater.* 2016, 62, 1–21.
[35] Niu WB, Li XL, Karuturi SK, Fam DW, Fan HJ, Shrestha S, Wong LH, Tok ALY. Applications of atomic layer deposition in solar cells. *Nanotechnology* 2015, 26, 064001.
[36] McDaniel MD, Ngo TQ, Hu S, Posadas A, Demkov AA, Ekerdt JG. Atomic layer deposition of perovskite oxides and their epitaxial integration with Si, Ge, and other semiconductors. *Appl. Phys. Rev.* 2015, 2, 041301.
[37] Tynell T, Karppinen M. Atomic layer deposition of ZnO: a review. *Semicond. Sci. Technol.* 2014, 29, 157–183.
[38] Wen L, Zhou M, Wang C, Mi Y, Lei Y. Energy storage: nanoengineering energy conversion and storage devices via atomic layer deposition. *Adv. Energy Mater.* 2016, 6, 1600468.
[39] Knoops HCM, Donders ME, van de Sanden MCM, Notten PHL, Kessels WMM. Atomic layer deposition for nanostructured Li-ion batteries. *J. Vac. Sci. Technol. A* 2012, 30, 010801.
[40] Hong K, Sang OK. Atomic layer deposition assisted sacrificial template synthesis of mesoporous TiO_2 electrode for high performance lithium ion battery anodes. *Energy Storage Mater.* 2015, 2, 27–34.
[41] Bai Y, Yan D, Yu C, Cao L, Wang C, Zhang J, Zhu H, Hu YS, Dai S, Lu J. Core-shell $Si@TiO_2$ nanosphere anode by atomic layer deposition for Li-ion batteries. *J. Power Sources* 2016, 308, 75–82.
[42] O'Neill BJ, Jackson DHK, Crisci AJ, Farberow CA, Shi F, Alba-Rubio AC, Lu J, Dietrich PJ, Gu X, Marshall CL. Stabilization of copper catalysts for liquid-phase reactions by atomic layer deposition. *Angew. Chem. Int. Ed.* 2013, 52, 13808–13812.
[43] Ramachandran RK, Dendooven J, Filez M, Galvita VV, Poelman H, Solano E, Minjauw MM, Devloocasier K, Fonda E, Hermidamerino D. Atomic layer deposition route to tailor nanoalloys of noble and non-noble metals. *ACS Nano* 2016, 10, 8770–8777.
[44] Yao Z, Wang C, Li Y, Kim N-Y. AAO-assisted synthesis of highly ordered, large-scale TiO_2 nanowire arrays via sputtering and atomic layer deposition. *Nanoscale Res. Lett.* 2015, 10, 166.
[45] Deng S, Kurttepeli M, Deheryan S, Cott DJ, Vereecken PM, Martens JA, Bals S, Van TG, Detavernier C. Synthesis of a 3D network of Pt nanowires by atomic layer deposition on a carbonaceous template. *Nanoscale* 2014, 6, 6939–6944.
[46] Woo JY, Han H, Kim JW, Lee SM, Ha JS, Shim JH, Han CS. Sub-5 nm nanostructures fabricated by atomic layer deposition using a carbon nanotube template. *Nanotechnology* 2016, 27, 265301.
[47] Borbón-Nuñez HA, Dominguez D, Muñoz-Muñoz F, Lopez J, Romo-Herrera J, Soto G, Tiznado H. Fabrication of hollow TiO_2 nanotubes through atomic layer deposition and MWCNT templates. *Powder Technol.* 2016, 308, 249–257.
[48] Ozgitakgun C, Kayaci F, Vempati S, Haider A, Celebioglu A, Goldenberg E, Kizir S, Uyar T, Biyikli N. Fabrication of flexible polymer–GaN core–shell nanofibers by the combination of electrospinning and hollow cathode plasma-assisted atomic layer deposition. *J. Mater. Chem. C* 2015, 3, 5199–5206.
[49] Ras RHA, Kemell M, De Wit J, Ritala M, Ten Brinke G, Leskelä M, Ikkala O. Hollow Inorganic nanospheres and nanotubes with tunable wall thicknesses by atomic layer deposition on self-assembled polymeric templates. *Adv. Mater.* 2006, 19, 102–106.
[50] Kayaci F, Vempati S, Ozgit-Akgun C, Donmez I, Biyikli N, Uyar T. Transformation of polymer-ZnO core–shell nanofibers into ZnO hollow nanofibers: intrinsic defect reorganization in ZnO and its influence on the photocatalysis. *Appl. Catal. B Environ.* 2015, 176, 646–653.
[51] Guan C, Wang X, Zhang Q, Fan Z, Zhang H, Fan HJ. Highly stable and reversible lithium storage in SnO_2 nanowires surface coated with a uniform hollow shell by atomic layer deposition. *Nano Lett.* 2014, 14, 4852–4858.
[52] Lotfabad EM, Kalisvaart P, Kohandehghan A, Cui K, Kupsta M, Farbod B, Mitlin D. Si nanotubes ALD coated with TiO_2, TiN or Al_2O_3 as high performance lithium ion battery anodes. *J. Mater. Chem. A* 2014, 2, 2504–2516.
[53] Guan C, Li X, Yu H, Mao L, Wong LH, Yan Q, Wang J. A novel hollowed CoO-in-$CoSnO_3$ nanostructure with enhanced lithium storage capabilities. *Nanoscale* 2014, 6, 13824–13830.
[54] Jin fan H, Knez M, Scholz R, Nielsch K, Pippel E, Hesse D, Zacharias M, Gosele U. Monocrystalline spinel nanotube fabrication based on the Kirkendall effect. *Nat. Mater.* 2006, 5, 627–631.
[55] Lee J, Farhangfar S, Yang R, Scholz R, Alexe M, Gösele U, Lee J, Nielsch K. A novel approach for fabrication of bismuth-silicon dioxide core-shell structures by atomic layer deposition. *J. Mater. Chem.* 2009, 19, 7050–7054.

[56] Qin Y, Pan A, Liu L, Moutanabbir O, Yang RB, Knez M. Atomic layer deposition assisted template approach for electrochemical synthesis of Au crescent-shaped half-nanotubes. *ACS Nano* 2011, 5, 788–794.
[57] Gu D, Baumgart H, Abdelfattah TM, Namkoong G. Synthesis of nested coaxial multiple-walled nanotubes by atomic layer deposition. *ACS Nano* 2010, 4, 753–758.
[58] Bae C, Zierold R, Moreno JMM, Kim H, Shin H, Bachmann J, Nielsch K. Multisegmented nanotubes by surface-selective atomic layer deposition. *J. Mater. Chem.* 2012, 1, 621–625.
[59] Karuturi SK, Cheng C, Liu L, Su LT, Fan HJ, Tok AIY. Inverse opals coupled with nanowires as photoelectrochemical anode. *Nano Energy* 2012, 1, 322–327.
[60] Kayaci F, Vempati S, Ozgit-Akgun C, Biyikli N, Uyar T. Enhanced photocatalytic activity of homoassembled ZnO nanostructures on electrospun polymeric nanofibers: a combination of atomic layer deposition and hydrothermal growth. *Appl. Catal. B* 156, 173–183.
[61] Cheng C, Zhang H, Ren W, Dong W, Sun Y. Three dimensional urchin-like ordered hollow TiO_2/ZnO nanorods structure as efficient photoelectrochemical anode. *Nano Energy* 2013, 2, 779–786.
[62] Guan C, Chao D, Wang Y, Wang J, Liu J. Confined Fe_2O_3 nanoparticles on graphite foam as high-rate and stable lithium-ion battery anode. *Part. Part. Syst. Charact.* 2016, 33, 487–492.
[63] Guan C, Wang Y, Hu Y, Liu J, Ho KH, Zhao W, Fan Z, Shen Z, Zhang H, Wang J. Conformally deposited NiO on a hierarchical carbon support for high-power and durable asymmetric supercapacitors. *J. Mater. Chem. A* 2015, 3, 23283–23288.
[64] Guan C, Qian X, Wang X, Cao Y, Zhang Q, Li A, Wang J. Atomic layer deposition of Co_3O_4 on carbon nanotubes/carbon cloth for high-capacitance and ultrastable supercapacitor electrode. *Nanotechnology* 2015, 26, 094001.
[65] Jang D, Meza LR, Greer F, Greer JR. Fabrication and deformation of three-dimensional hollow ceramic nanostructures. *Nat. Mater.* 2013, 12, 893–898.
[66] Werner JG, Scherer MRJ, Steiner U, Wiesner U. Gyroidal mesoporous multifunctional nanocomposites via atomic layer deposition. *Nanoscale* 2014, 6, 8736–8742.
[67] Rolison DR, Long JW, Lytle JC, Fischer AE, Rhodes CP, McEvoy TM, Bourg ME, Lubers AM. Multifunctional 3D nanoarchitectures for energy storage and conversion. *Chem. Soc. Rev.* 2009, 38, 226–252.
[68] Marichy C, Pinna N. Carbon-nanostructures coated/decorated by atomic layer deposition: growth and applications. *Coord. Chem. Rev.* 2013, 257, 3232–3253.
[69] Hsieh CT, Chen WY, Tzou DY, Roy AK, Hsiao HT. Atomic layer deposition of Pt nanocatalysts on graphene oxide nanosheets for electro-oxidation of formic acid. *Int. J. Hydrogen Energy* 2012, 37, 17837–17843.
[70] Lee HB, Baeck SH, Jaramillo TF, Bent SF. Growth of Pt nanowires by atomic layer deposition on highly ordered pyrolytic graphite. *Nano Lett.* 2013, 13, 457–463.
[71] Oh IK, Tanskanen J, Jung H, Kim K, Mi JL, Lee Z, Lee SK, Ahn JH, Chang WL, Kim K. Nucleation and growth of the HfO_2 dielectric layer for graphene-based devices. *Chem. Mater.* 2015, 27, 5868–5877.
[72] Marichy C, Tessonnier JP, Ferro MC, Lee KH, Schlögl R, Pinna N, Willinger MG. Labeling and monitoring the distribution of anchoring sites on functionalized CNTs by atomic layer deposition. *J. Mater. Chem.* 2012, 22, 7323–7330.
[73] Zhu H, Mcdonnell S, Qin X, Azcatl A, Cheng L, Addou R, Kim J, Ye PD, Wallace RM. Al2O3 on black phosphorus by atomic layer deposition: an in situ interface study. *ACS Appl. Mater. Interfaces* 2015, 7, 13038–13043.
[74] Silva RM, Ferro MC, Araujo JR, Achete CA, Clavel G, Rui FES, Pinna N. Nucleation, growth mechanism, and controlled coating of ZnO ALD onto vertically aligned N-doped CNTs. *Langmuir* 2016, 32, 7038–7044.
[75] Stambula S, Gauquelin N, Bugnet M, Gorantla S, Turner S, Sun S, Liu J, Zhang G, Sun X, Botton GA. Chemical structure of nitrogen-doped graphene with single platinum atoms and atomic clusters as a platform for the PEMFC electrode. *J. Phys. Chem. C* 2014, 118, 3890–3900.
[76] Dameron AA, Pylypenko S, Bult JB, Neyerlin KC, Engtrakul C, Bochert C, Leong GJ, Frisco SL, Lin S, Dinh HN. Aligned carbon nanotube array functionalization for enhanced atomic layer deposition of platinum electrocatalysts. *Appl. Surf. Sci.* 2012, 258, 5212–5221.
[77] Pirkle A, Mcdonnell S, Lee B, Kim J, Colombo L, Wallace RM. The effect of graphite surface condition on the composition of Al_2O_3 by atomic layer deposition. *Appl. Phys. Lett.* 2010, 97, 082901.
[78] Shin WC, Bong JH, Choi SY, Cho BJ. Functionalized graphene as an ultrathin seed layer for the atomic layer deposition of conformal high-k dielectrics on graphene. *ACS Appl. Mater. Interfaces* 2013, 5, 11515–11519.
[79] Meng X, Ionescu M, Banis MN, Zhong Y, Liu H, Zhang Y, Sun S, Li R, Sun X. Heterostructural coaxial nanotubes of CNT@Fe_2O_3 via atomic layer deposition: effects of surface functionalization and nitrogen-doping. *J. Nanopart. Res.* 2011, 13, 1207–1218.
[80] Zheng L, Cheng X, Yu Y, Xie Y, Li X, Wang Z. Controlled direct growth of Al_2O_3-doped HfO_2 films on graphene by H_2O-based atomic layer deposition. *Phys. Chem. Chem. Phys.* 2015, 17, 3179–3185.
[81] Han KS, Kalode PY, Koo Lee YE, Kim H, Lee L, Sung MM. A non-destructive n-doping method for graphene with precise control of electronic properties via atomic layer deposition. *Nanoscale* 2016, 8, 5000–5005.
[82] Boichot R, Tian L, Richard MI, Crisci A, Chaker A, Cantelli V, Coindeau S, Lay S, Ouled T, Guichet C. Evolution of crystal structure during the initial stages of ZnO atomic layer deposition. *Chem. Mater.* 2016, 28, 592–600.
[83] Farmer DB, Gordon RG. Atomic layer deposition on suspended single-walled carbon nanotubes via gas-phase noncovalent functionalization. *Nano Lett.* 2006, 6, 699–703.
[84] Young MJ, Musgrave CB, George SM. Growth and characterization of Al_2O_3 atomic layer deposition films on sp^2-graphitic carbon substrates using NO_2/trimethylaluminum pretreatment. *ACS Appl. Mater. Interfaces* 2015, 7, 12030–12037.
[85] Bielinski AR, Kazyak E, Schlepütz CM, Jung HJ, Wood KN, Dasgupta NP. Hierarchical ZnO nanowire growth with tunable orientations on versatile substrates using atomic layer deposition seeding. *Chem. Mater.* 2015, 27, 4799–4807.
[86] Weber MJ, Verheijen MA, Bol AA, Kessels WM. Sub-nanometer dimensions control of core/shell nanoparticles prepared by atomic layer deposition. *Nanotechnology* 2015, 26, 094002.

[87] Lu J, Low KB, Lei Y, Libera JA, Nicholls A, Stair PC, Elam JW. Toward atomically-precise synthesis of supported bimetallic nanopoarticles using atomic layer deposition. *Nat. Commun.* 2014, 5, 3264.
[88] Yanguas-Gil A, Peterson KE, Elam JW. Controlled dopant distribution and higher doping efficiencies by surface-functionalized atomic layer deposition. *Chem. Mater.* 2011, 23, 4295–4297.
[89] Jiang X, Bent SF. Area-selective ALD with soft lithographic methods: using self-assembled monolayers to direct film deposition. *J. Phys. Chem. C* 2009, 113, 17613–17625.
[90] Kung H, Teplyakov AV. Formation of copper nanoparticles on ZnO powder by a surface-limited reaction. *J. Phys. Chem. C* 2014, 118, 1990–1998.
[91] Ray NA, Duyne RPV, Stair PC. Synthesis strategy for protected metal nanoparticles. *J. Mater. Chem. C* 2012, 116, 7748–7756.
[92] Feng H, Lu J, Stair PC, Elam JW. Alumina over-coating on Pd nanoparticle catalysts by atomic layer deposition: enhanced stability and reactivity. *Catal. Lett.* 2011, 141, 512–517.
[93] Cheng N, Banis MN, Liu J, Riese A, Li X, Li R, Ye S, Knights S, Sun X. Extremely stable platinum nanoparticles encapsulated in a zirconia nanocage by area-selective atomic layer deposition for the oxygen reduction reaction. *Adv. Mater.* 2015, 27, 277–281.
[94] Cao K, Zhu Q, Shan B, Chen R. Controlled synthesis of Pd/Pt core shell nanoparticles using area-selective atomic layer deposition. *Sci. Rep.* 2015, 5, 8470.
[95] Minaye Hashemi FS, Prasittichai C, Bent SF. Self-correcting process for high quality patterning by atomic layer deposition. *ACS Nano* 2015, 9, 8710–8717.
[96] Chopra SN, Zhang Z, Kaihlanen C, Ekerdt JG. Selective growth of titanium nitride on HfO_2 across nanolines and nanopillars. *Chem. Mater.* 2016, 28, 4928–4934.
[97] Dong W, Zhang K, Zhang Y, Wei T, Sun Y, Chen X, Dai N. Application of three-dimensionally area-selective atomic layer deposition for selectively coating the vertical surfaces of standing nanopillars. *Sci. Rep.* 2014, 4, 4458.
[98] Färm E, Kemell M, Ritala M, Leskelä M. Selective-area atomic layer deposition with microcontact printed self-assembled octadecyltrichlorosilane monolayers as mask layers. *Thin Solid Films* 2008, 517, 972–975.
[99] Hua Y, King WP, Henderson CL. Nanopatterning materials using area selective atomic layer deposition in conjunction with thermochemical surface modification via heated AFM cantilever probe lithography. *Microelectron. Eng.* 2008, 85, 934–936.
[100] Huang J, Lee M, Lucero A, Cheng L, Kim J. Area-selective ALD of TiO_2 nanolines with electron-beam lithography. *J. Phys. Chem. C* 2014, 118, 23306–23312.
[101] Choi KH, Ali K, Chang YK, Muhammad NM. Characterization of Al_2O_3 thin films fabricated at low temperature via atomic layer deposition on pen substrates. *Chem. Vapor Depos.* 2014, 20, 118–124.
[102] Kim H, Lee HBR, Maeng WJ. Applications of atomic layer deposition to nanofabrication and emerging nanodevices. *Thin Solid Films* 2009, 517, 2563–2580.
[103] Profijt HB, Potts SE, Van dS, M. C. M., Kessels WMM. Plasma-assisted atomic layer deposition: basics, opportunities, and challenges. *J. Vac. Sci. Technol. A* 2011, 29, 050801.
[104] Ji S, Cho GY, Yu W, Su PC, Lee MH, Cha SW. Plasma-enhanced atomic layer deposition of nanoscale yttria-stabilized zirconia electrolyte for solid oxide fuel cells with porous substrate. *ACS Appl. Mater. Interfaces* 2015, 7, 2998–3002.
[105] Assaud L, Pitzschel K, Hanbücken M, Santinacci L. Highly-conformal TiN thin films grown by thermal and plasma-enhanced atomic layer deposition. *ECS J. Solid State Sci. Technol.* 2014, 3, 253–258.
[106] Minjauw MM. Near room temperature plasma enhanced atomic layer deposition of ruthenium using the RuO_4-precursor and H_2-plasma. *J. Mater. Chem. C* 2015, 3, 4848–4851.
[107] Rampelberg G, Longrie D, Deduytsche D. Plasma enhanced atomic layer deposition on powders. *ECS Trans.* 2014, 64, 51–62.
[108] Schindler P, Kim Y, Thian D, An J, Prinz FB. Plasma-enhanced atomic layer deposition of $BaTiO_3$. *Scripta Mater.* 2016, 111, 106–109.
[109] Kariniemi M, Niinistö J, Hatanpää T, Kemell M, Sajavaara T, Ritala M, Leskelä M. Plasma-enhanced atomic layer deposition of silver thin films. *Chem. Mater.* 2011, 23, 2901–2907.
[110] Deduytsche D, Poelman H, Meirhaeghe RV, Berghe SVD, Detavernier C, Musschoot J, Haemers J. Comparison of thermal and plasma enhanced ALD/CVD of vanadium pentoxide. *J. Electrochem. Soc.* 2009, 156, 122–126.
[111] Duan CL, Deng Z, Cao K, Yin HF, Shan B, Chen R. Surface passivation of Fe_3O_4 nanoparticles with Al_2O_3 via atomic layer deposition in a rotating fluidized bed reactor. *J. Vac. Sci. Technol. A* 2016, 34, 04C103.
[112] Didden A, Hillebrand P, Wollgarten M, Dam B, Krol RVD. Deposition of conductive TiN shells on SiO_2 nanoparticles with a fluidized bed ALD reactor. *J. Nanopart. Res.* 2016, 18, 1–11.
[113] Didden AP, Middelkoop J, Besling WFA, Nanu DE, Roel VDK. Fluidized-bed atomic layer deposition reactor for the synthesis of core-shell nanoparticles. *Rev. Sci. Instrum.* 2014, 85, 013905–013905.
[114] Scheffe JR, Francés A, King DM, Liang X, Branch BA, Cavanagh AS, George SM, Weimer AW. Atomic layer deposition of iron(III) oxide on zirconia nanoparticles in a fluidized bed reactor using ferrocene and oxygen. *Thin Solid Films* 2009, 517, 1874–1879.
[115] Lu J, Stair PC. Nano/subnanometer Pd nanoparticles on oxide supports synthesized by AB-type and low-temperature ABC-type atomic layer deposition: growth and morphology. *Langmuir* 2010, 26, 16486–16495.
[116] Masango SS, Peng L, Marks LD, Duyne RPV, Stair PC. Nucleation and growth of silver nanoparticles by AB and ABC-type atomic layer deposition. *J. Phys. Chem. C* 2014, 118, 17655–17661.
[117] Kalutarage LC, Clendenning SB, Winter CH. Low-temperature atomic layer deposition of copper films using borane dimethylamine as the reducing co-reagent. *Chem. Mater.* 2014, 26, 3731–3738.
[118] Zhou Y, King DM, Liang X, Li J, Weimer AW, Zhou Y, King DM, Weimer AW. Optimal preparation of Pt/TiO_2 photocatalysts using atomic layer deposition. *Appl. Catal. B Environ.* 2010, 101, 662–664.
[119] Lu J, Elam JW. Low Temperature ABC-type Ru ALD through consecutive dissociative chemisorption, combustion and reduction steps. *Chem. Mater.* 2015, 27, 4950–4956.
[120] Mattinen M, Hämäläinen J, Vehkamäki M, Heikkilä MJ, Mizohata K, Jalkanen P, Räisänen J, Ritala M, Leskelä M. Atomic layer deposition of iridium thin films using sequential oxygen

and hydrogen pulses. *J. Phys. Chem. C* 2016, 120, 15235–15243.
[121] Mackus AJM, Leick N, Baker L, Kessels WMM. Catalytic combustion and dehydrogenation reactions during atomic layer deposition of platinum. *Chem. Mater.* 2012, 24, 1752–1761.
[122] Knisley TJ, Ariyasena TC, Sajavaara T, Saly MJ, Winter CH. Low temperature growth of high purity, low resistivity copper films by atomic layer deposition. *Chem. Mater.* 2011, 23, 4417–4419.
[123] Dey G, Elliott SD. Copper reduction and atomic layer deposition by oxidative decomposition of formate by hydrazine. *RSC Adv.* 2014, 4, 34448–34453.
[124] Bielinski AR, Dasgupta NP. Atomic layer deposition of core-shell nanowires for solar energy conversion devices. *ECS Trans.* 2015, 69, 3–13.
[125] Lim JY, Pezeshki A, Oh S, Kim JS, Lee YT, Yu S, Hwang DK, Lee G-H, Choi HJ, Im S. Homogeneous 2D $MoTe_2$ p–n junctions and CMOS inverters formed by atomic-layer-deposition-induced doping. *Adv. Mater.* 2017, 1701798.
[126] Wang X, Zhang T-B, Yang W, Zhu H, Chen L, Sun Q-Q, Zhang DW. Improved integration of ultra-thin high-k dielectrics in few-layer MoS_2 FET by remote forming gas plasma pretreatment. *Appl. Phys. Lett.* 2017, 110, 053110.
[127] Mahuli N, Sarkar SK. Atomic layer deposition of NiS and its application as cathode material in dye sensitized solar cell. *J. Vac. Sci. Technol. A* 2016, 34, 01A142.
[128] Wen L, Mi Y, Wang C, Fang Y, Grote F, Zhao H, Zhou M, Lei Y. Cost-effective atomic layer deposition synthesis of pt nanotube arrays: application for high performance supercapacitor. *Small* 2014, 10, 3162–3168.
[129] Mousa MBM, Oldham CJ, Parsons GN. Precise nanoscale surface modification and coating of macroscale objects: open-environment in loco atomic layer deposition on an automobile. *ACS Appl. Mater Interfaces* 2015, 7, 19523–19529.
[130] Munoz-Rojas D, MacManus-Driscoll J. Spatial atmospheric atomic layer deposition: a new laboratory and industrial tool for low-cost photovoltaics. *Mater. Horiz.* 2014, 1, 314–320.

Bionotes

Liang Hu
School of Materials Science and Engineering, Central South University, Changsha, Hunan 410083, China

Liang Hu has currently a Master's degree in the School of Materials Science and Engineering, Central South University of China. He received his Bachelor's degree from the School of Materials Science and Engineering, Wuhan University of Technology in 2015. His research focuses on atomic layer deposition.

Weihong Qi
School of Materials Science and Engineering, Central South University, Changsha, Hunan 410083, China
weihong.qi@gmail.com; qiwh216@csu.edu.cn

Weihong Qi is a full professor at Central South University. He received his PhD degree in Materials Physics from Central South University in 2004 and was a Research Fellow at the City University of Hong Kong from 2009 to 2010. His research interests include functional nanoalloys and 2D materials, thermodynamics of low-dimensional solids and computational materials science. He has served as a director of the Micron-Nano Society of China and is a review expert for the National Natural Science Foundation of China. He was also a lead guest editor for the Journal of Nanomaterials and has been invited to serve as a reviewer for more than 30 journals.

Yejun Li
Hunan Key Laboratory of Super Microstructure and Ultrafast Process, School of Physics and Electronics, Central South University, Changsha, Hunan 410083, China

Yejun Li is currently a lecturer in the School of Physics and Electronics, Central South University, China. He received his Bachelor's and Master's degrees from the School of Materials Science and Engineering, Central South University in 2008 and 2012, respectively. In 2016, he received his PhD degree from the Department of Physics and Astronomy, KU Leuven, Belgium. His research focuses on laser spectroscopy of 2D materials, metallic nanoparticle and clusters, and atomic layer deposition on these systems.